An Investigation Into the Use of Orthogonal Frequency Division Multiplexing in Packet Radio

by

Rob Neilson

National Higher Diploma *Technikon Witwatersrand*

Submitted to the Department of Electrical Engineering
in partial fulfillment of the requirements for the degree of
Master of Science in Electrical Engineering
at the
UNIVERSITY OF CAPE TOWN
March 2005

Signature of Author ..... Signed by candidate .....

R. G. Neilson
Department of Electrical Engineering
26 February 2005

Certified by .....

Prof. G de Jager
Supervisor

Declaration

I declare that this dissertation is my own work and is being submitted in partial fulfillment of the requirements for the degree of Master of Science in Electrical Engineering. It has not been submitted for any degree at this or any other institution. All consulted literature has been listed in the references.

R. G. Neilson
Candidate

Acknowledgements

I would like to thank Prof. Gerhard de Jager for taking over the supervision of this thesis. I would also like to thank Dr. Robin Braun for his initial supervision and to DR Johan van de Groenendaal for his help in the initial stages of the project.

I would like to give a special thank you to two of my colleagues, Clive Whaits and Egon Voss. To Egon for his help in my early university mathematics career, I would never have made it without your help, and to Clive for his academic support throughout my time at the Cape Technikon. Most importantly I would like to thank both of them for their unwavering friendship and support through some difficult personal times.

Lastly I would like to thank my family for their patience and support. OK guys, now you can have the computer all to yourselves.

Synopsis

The concept of Orthogonal Frequency Division Multiplexing has been around since the 1960s. It has resurfaced over the last decade as being the modulation scheme of choice in some newer technologies like Digital Video Broadcasting (DVB) and Asynchronous Digital Subscriber lines (ADSL). Amateur packet radio started in 1978 and has attracted thousands of enthusiasts from around the world. The interest in packet radio has waned over the years due advances in the data transmission capabilities of landline systems and also more widespread access to the Internet.

The purpose of this thesis was to develop a simple software simulation model to determine whether or not OFDM could be used to increase the data rates currently available in packet radio systems.

The thesis starts out with an introduction to packet radio and OFDM in Chapter 1. A slightly more detailed discussion on OFDM is given in Chapter 2 in order to develop a basic specification for the proposed OFDM model. Chapters 2,3 and 4 discuss the development of the Transmitter model, the Receiver model and the Channel model respectively using the Simulink software package. Chapter 6 discusses the problem of Peak-to-Average Power Ratios (PAPR) in OFDM and explores the use of A-law companding to reduce this problem. In Chapter 7, the developed models are simulated and their performance compared to theoretical expectations. The full system is also simulated in this chapter in order to ascertain the possible data rate through the modelled packet radio channel. Conclusions regarding the application of OFDM to packet radio are presented in Chapter 8.

Table of Contents

List of Figures

List of Tables

List of Abbreviations

ADSL	Asymmetric Digital Subscriber Lines
AFSK	Audio Frequency Shift Keying
AWGN	Additive White Gaussian Noise
bps	Bits per second
DAB	Digital Audio Broadcasting
DFT	Discrete Fourier Transform
DLL	Digital Phase Locked Loop
DVB	Digital Video Broadcasting
FEC	Forward Error Correction
FHSS	Frequency Hopped Spread Spectrum
FSK	Frequency Shift Keying
GUI	Graphical User Interface
HF	High Frequency
ISI	Inter-symbol Interference
ISM	Industrial, Scientific and Medical
IVOC	Interactive Video on Demand
MCM	Multi-Carrier Modulation
MSK	Minimum Shift Keying
NBFM	Narrow Band Frequency Modulation
OFDM	Orthogonal Frequency Division Multiplexing
OSI	Open Systems Interconnection Reference Model
PAPR	Peak-to-Average Power Ratio
PSTN	Public Switched Telephone Network
QAM	Quadrature Amplitude Modulation
QPSK	Quadrature Phase Shift Keying
RF	Radio Frequency

rms	Root Mean Square
SER	Symbol Error Rate
SNR	Signal-to-Noise Ratio
TNC	Terminal Node Controller
TAPR	Tucson Amateur Packet Radio Corporation
VADCG	Vancouver Amateur Digital Communication Group
WLAN	Wireless Local Area Network

Chapter 1

Introduction

Experimenters in the amateur packet radio field have been experimenting with the transmission of digital information via commercially available communications equipment for almost three decades. This chapter gives a brief history of packet radio and discusses a number of packet radio systems that are currently in use. A brief introduction to Orthogonal Frequency Division Multiplexing (OFDM) is also given and the chapter closes by presenting a standard OFDM system model that will be used to investigate the use of multi-carriers in a basic packet radio environment.

1.1 Amateur Packet Radio

1.1.1 A Brief History

Amateur packet radio began in 1978 in Montreal Canada [1]. The Vancouver Amateur Digital Communication Group (VADCG) developed the first Terminal Node Controller (TNC), a device required for the handling of packet data, in 1980. The TNC standard currently in use was developed after a meeting of the Tucson chapter of the IEEE Computer Society in 1981.Further discussions led to the investigation of the feasibility of the development of a TNC that could be used by amateur radio enthusiasts. The Tucson Amateur Packet Radio Corporation (TAPR) was formed for this project. The first TAPR TNC was used on 26th June 1982 to initiate data communications using amateur radio equipment. Over the years the TNC-2 was

developed, and this has become the most commonly used controller for packet radio worldwide.

1.1.2 Basic Operation

To explain the basic operation of amateur packet radio we can make a simple comparison to the transfer of data between two computers connected via modems to the Public Switched Telephone Network (PSTN). The data from one computer (or terminal) is sent to the modem where it is converted into a format suitable for transmission over the public telephone lines. In a packet radio system, the telephone modem is replaced by a device called a terminal node controller (TNC), the telephone connection to the PSTN is replaced by an amateur radio transceiver, and the PSTN is replaced by the amateur radio waves. Packet radio takes the data stream from the

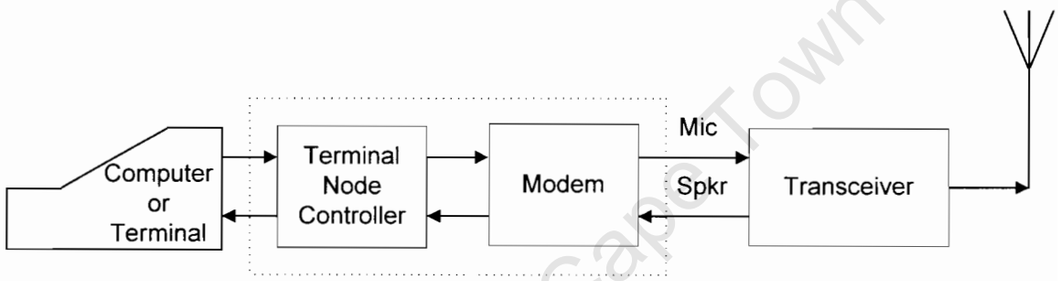

Figure 1.1: Block Diagram of a Packet-Radio Station

computer and sends this data, in short bursts or packets, via radio to another station that is equipped for receiving the data [1]. The block diagram of a typical packet-radio station is shown in Figure 1.1 [2].

A packet-radio station is made up of a number of distinct elements :

Terminal Node Controller (TNC)

The TNC is responsible for the assembly and disassembly of the digital information into packets and for the control of data flow between the user and the radio transceiver. During transmission, the TNC will divide the data into packets and will automatically key the transmitter when the packets are ready for transmission. During reception, the TNC decodes the received packets, checks for errors, and passes the received data on to the host computer or terminal. The TNC can also be used as packet relay station which is sometimes referred to as a digipeater.

Computer or Terminal

This is the interface between the user and the system. The computer must be equipped with software that can deal with data packets. Most phone modem communications programs can be adapted for use with packet radio.

Transceiver

This is the link to other packet radio stations using radio frequency (RF) signals. Commercially available narrow band FM voice radios can be used for data rates of 1200/2400 bits per second (bps). For higher data rates (9600 bps and greater), special equipment or modified FM radios must be used. The most common packet radio is used with 1200 bps audio frequency shift keying (AFSK) TNCs in the 2m band (144 MHz - 148 MHz) [1].

1.2 Packet Radio Standards

Wherever possible, packet radio has adopted standards that have been laid down by the communications industry. This has the benefit of maintaining a high degree of compatibility with industry standards and ensures that the transfer of digital information can take place between communications equipment of differing origins. Under these conditions, the data communication is a transparent, or open, process.

A standard that has been adopted for data communications worldwide is the Open Systems Interconnection Reference Model (OSI model, also referred to as OSRIM) [3]. This model supplies a framework for data communications that makes use of standard interconnection protocols between the various elements, or layers, of the model. The layers are essentially independent of each other since they are not configured for a specific system architecture or implementation. What is required is that the layers perform a well-defined set of functions and that similar functions are assigned to the same layer. The structure of the OSI model is illustrated in Figure 1.2:

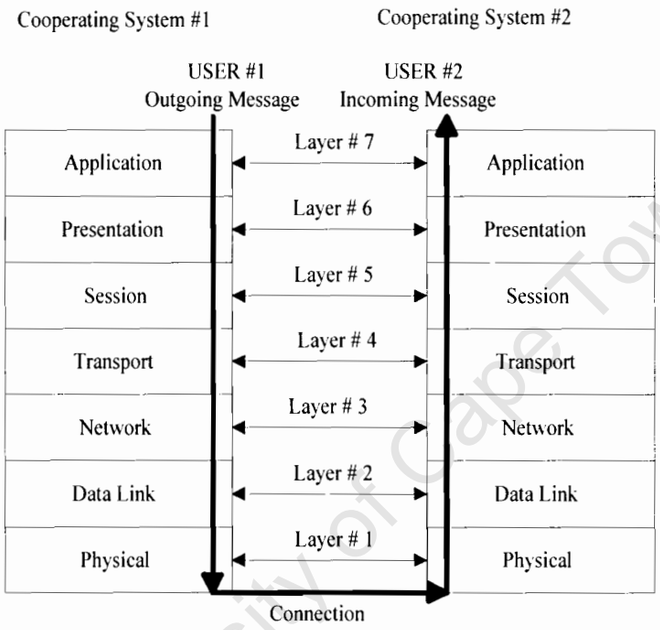

Figure 1.2: The Open Systems Interconnection Reference Model

The functions of the various layers shown in Figure 1.2 are defined by the layer standard. An in depth discussion o the OSI model can be found in most texts dealing with computer networking or data communications [3]. Two specific layers, namely, the Data Link Layer and the Physical Layer, will be mentioned here in connection with the transmission of packet data using radio equipment.

1.2.1 Data Link Layer (Layer 2)

This layer arranges the data bits into frames. The most common protocol used is the International Organization for Standards (ISO) High-Level Data Link Control (HDLC). This layer establishes a link (via radio) through the use of supervisory frames. It is also responsible for error detection and recovery [2]. The so-called AX.25 or amateur X.25 protocol is used at this level in amateur packet radio systems.

1.2.2 Physical Layer (Layer 1)

This layer is concerned with the actual transmission and reception of the data bit-streams between users. The physical layer defines the electrical and mechanical standards required for the type of communications media and communications equipment used [3]. Modems, radio equipment and the type of media (twisted pairs, radio links etc) over which the communications process takes place, are all layer 1 considerations.

1.3 Equipment Options for Packet Radio

Packet radio requires that the digital information from the computer be converted into a form that is suitable for transmission using radio communications equipment. The TNC assembles the digital information into blocks or packets but a modem is required for the conversion of the data into a form that can be transmitted by the radio equipment [4]. A number of different equipment options are available [5], but this section will specifically discuss the G3RUH modem and the WA4DSY modem since both modems have been available to amateur radio enthusiasts in kit form for over a decade and some are still in use up to the present time.

1.3.1 The G3RUH Modem

Two modems will be considered in this section :

- The K9NG modem.
- The G3RUH modem.

The K9NG modem was a means of getting started in packet radio at a reasonable cost. This modem was available in kit form from TAPR for a number of years and set the "standard" for 9600 bps packet operation [5]. The modem used a frequency shift keying (FSK) scheme for the transmission of the data. The K9NG modem was replaced by the G3RUH modem and later TAPR designs. The modem was designed by James Miller, G3RUH. The modem featured full duplex operation and could be used with a wide range of voice grade narrow band FM (NBFM) radios after implementing a number of minor modifications [6]. The modem featured a 20 kHz RF spectrum, digital generation of the transmit audio, waveform shaping to compensate for the amplitude and phase response of the receiver, and a digital phase locked loop (DLL) circuit. A number of modifications were later suggested by James Miller in order to increase the data throughput of the modem to a maximum of 64 kbps [7].

1.3.2 The WA4DSY RF Modem

In 1987 Dale Heatherington presented a paper that described the development of a 56 kilobaud synchronous RF modem with a 70 kHz bandwidth [8]. The modulation scheme used was band-limited minimum frequency shift keying (MSK) generated by a digital state machine using two digital-to-analogue converters and two double balanced modulators. Demodulation was accomplished using a standard quadrature detector chip. In 1995 the modem was redesigned in order to improve reliability and reduce the cost and size of the modem [9]. Most of the modem functions were implemented using a Field Programmable Gate Array (FPGA). The MSK signal was digitally generated to eliminate the need for the analogue modulators and phase shifters. The data rate for the modem was fixed at 56 kbps. The modem is a true modem in the sense that the RF modulation and demodulation circuitry is built into the modem i.e. there is no need for external RF radio equipment.

1.3.3 Packet Modem Developments

As Internet access becomes cheaper and faster, the interest and participation in high-speed digital packet radio is decreasing [10]. Most amateurs consider it unnecessary to implement high-speed packet radio systems, especially since many landline modems can offer data rates similar to that of currently available RF modems. What has redirected interest in high-speed packet radio of late is the advent of spread spectrum (SS) wireless local area networks (WLAN), since the hardware can be used without a licence in some of the ISM bands.

TAPR has been involved in the development of a unit capable of transmitting high speed packet data using spread spectrum techniques [11]. The system is intended for use in the 900 MHz amateur band (902-928 MHz). The design is based on frequency-hopped spread spectrum (FHSS). The system also makes use of forward error correction (FEC) and quadrature phase shift keying (QPSK) modulation. Some of the general requirements are that the unit provide at least a 128 kbps data rate while providing a 20 mile coverage using a 1 watt transmitter. The unit should also provide for direct connection to the LAN port of a laptop or personal computer. Areas of application include audio conferencing and mobile laptop video-conferencing.

1.4 Multi-Carrier Modulation (MCM)

1.4.1 A Brief History

This modulation scheme has been known as Discrete Multi-tone (DMT) modulation, Multi-carrier modulation (MCM) and more recently as Orthogonal Frequency Division Multiplexing (OFDM). Multiple carrier techniques can be traced back to Chang in the 1960's [12][13]. The basic idea behind DMT is to split the available channel bandwidth into a number of sub-channels. Each of these sub-channels is assigned a carrier. If these carriers are orthogonal, then a certain amount of spectral

overlap can occur, thereby increasing the overall throughput of the channel. Such a system was referred to as a "parallel" data system. For large numbers of sub-carriers the required number of modulators and demodulators required expensive and complex systems. Weinstein and Ebert applied the Discrete Fourier Transform (DFT) to the system in order to reduce system complexity and combat ISI [14]. Hirosaki explored the use of the DFT to produce a set of multiplexed quadrature amplitude modulated (QAM) carriers [15][16]. Kalet [33] looked at the maximisation of the bit rate using QAM. There is a vast amount of literature available that covers the development of OFDM systems over the last few decades.

1.4.2 Areas of Application

Early areas of application were to data modems for HF radio [16]. Due to the complexity of early systems the application of OFDM seemed to be limited, but with recent developments (late 90's onwards) in high speed digital signal processing techniques, OFDM has been used in a number of newer applications, including the following [17][18]:

- Digital Audio Broadcasting (DAB)
- Digital Terrestrial Television (Video) Broadcasting (DVB)
- Asymmetric Digital Subscriber Lines (ADSL)
- Interactive Video on Demand (IVOD)

Although the OFDM technique has been applied to a number of communications systems it has never been applied directly to amateur packet radio systems in order to increase data rates. The purpose of this thesis is to develop a simulation model that can be used to investigate the application of this technique to packet radio. A full description of a general OFDM system will follow in Chapter 2.

Chapter 2

A General OFDM System

This chapter presents the block diagram of a general OFDM system based on the use of the Fast Fourier Transform (FFT). The discussion also includes a basic specification that was applied to the software model used for the investigation into the use of OFDM in packet radio. This basic model was used as the platform for the development of a simulation model using Simulink.

2.1 Basic Operation and Block Diagram

2.1.1 Orthogonal Carriers

The operation of the system is based on the paper by Bingham [19]. In the introduction it was mentioned that the basic idea behind OFDM is to divide an existing channel up into a number of smaller sub-channels. Each of these sub-channels is assigned a carrier and if the frequency spacing between the carriers is correctly chosen then the frequency spectra of the modulated carriers can overlap without any inter carrier interference. This is illustrated graphically in Figure 2.1.

Figure 2 shows the frequency spectrum for 2 modulated carriers with rectangular pulse shaping. If the spacing between the carriers is the same as the symbol rate, adjacent carriers will not interfere. When one of the carriers is at is maximum value, the others will be at zero magnitude, as indicated by points A and B in the figure.

Even though the signal spectra overlap, the original carriers and data can still be recovered. This is a very simplified explanation of the basic principle behind OFDM.

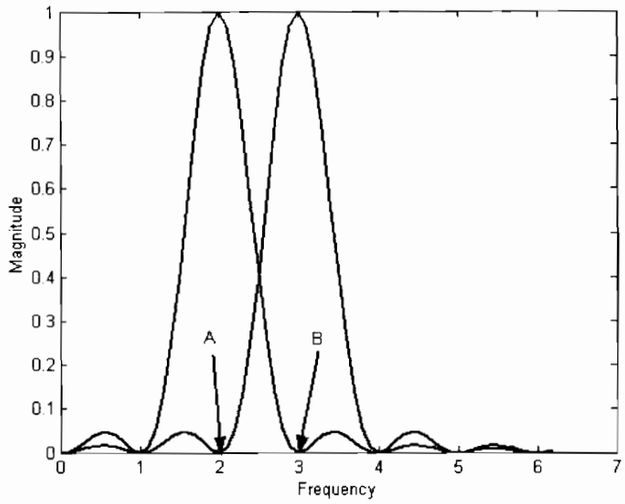

Figure 2.1: Frequency Spectrum for Orthogonal Carriers

2.1.2 Block Diagram

The block diagram for a general OFDM system is shown in Figure 2.2.

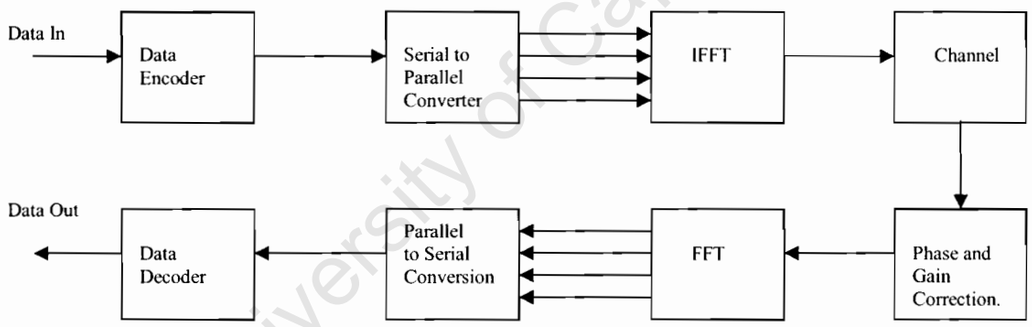

Figure 2.2: Block Diagram of a General OFDM System

The basis behind the operation of this system lies in the use of the DFT, implemented as a FFT, to generate and demodulate the required multitone data signals. In [14] it is shown that the required OFDM signal is effectively the Inverse Fourier Transform of the original data and the Fourier Transform is effectively a bank of coherent

demodulators that can be used to recover the original data. Mathematically the transmitted OFDM signal is the real part of the IFFT (or FFT). This is shown in (2.1).

$$f(t) = \mathrm{Re}\left[\frac{1}{N}\sum_{n=0}^{N-1} d(n)e^{j\omega_n t}\right] \qquad (2.1)$$

where N is equal to the number of carriers in the system and $d(n)$ is the required data stream. By truncating the signal to the interval $(0, N\Delta t)$, where $t_s = \frac{1}{f_s}$ and f_s is the symbol rate, the signal has a $\frac{\sin x}{x}$ spectral density that maintains an orthogonal set of carriers [19]. The FFT (or IFFT) is used in the receiver to recover the original data by applying the reverse process to the OFDM signal.

2.2 System Model Specification

2.2.1 Available Bandwidth

The available bandwidth for transceivers used in packet radio is approximately 8 kHz [6][7]. Measurements carried out on an Agilent Technologies RF Communication Test Set, HP8920A, confirm this. These measurements are discussed in detail in Chapter 4, which deals with the channel model.

2.2.2 Modulation Scheme

The type of carrier modulation scheme determines the spectral characteristics of the modulated signal. The modulation scheme chosen was 16-ary quadrature amplitude modulation (16-QAM). The reasons for this are given in [20] and are summarized as follows:

- 16QAM has a low value of signal-to-noise ratio (SNR) for a given probability of error.
- The scheme has good spectrum utilization.

- Rectangular constellation permits ease of implementation in both the receiver and transmitter.

2.2.3 Number of Carriers

The number of carriers in the system is a function of the available bandwidth and the carrier spacing. The number of carriers can be calculated as follows:

$$N = \frac{f_{BW} - \Delta f}{\Delta f} \tag{2.2}$$

where f_{BW} is the available channel bandwidth and Δf is the frequency spacing between carriers and is normally equal to the symbol rate f_s.

A simple Matlab program, *tones.m*, was written to select a number (3900 in total) of possible symbol rates and determine the overall data throughput for the system. A program listing can be found in Appendix A. The graph in Figure 2.3 shows the possible data rates versus the number of carriers using 16QAM modulation (4 bits per symbol) with an available bandwidth of 8 kHz.

The maximum data rate for the system was 32 kbps with $N = 80$. This would give a frequency spacing of 100 Hz and a symbol period of 10 ms. A consideration for this specification would be whether or not the system could be implemented on a standard DSP development kit. Since 16-QAM was being used, the receiver would have to calculate 16 distance metrics for each carrier in order to demodulate the received information. These calculations would have to be carried out, along with the FFT, within the symbol period.

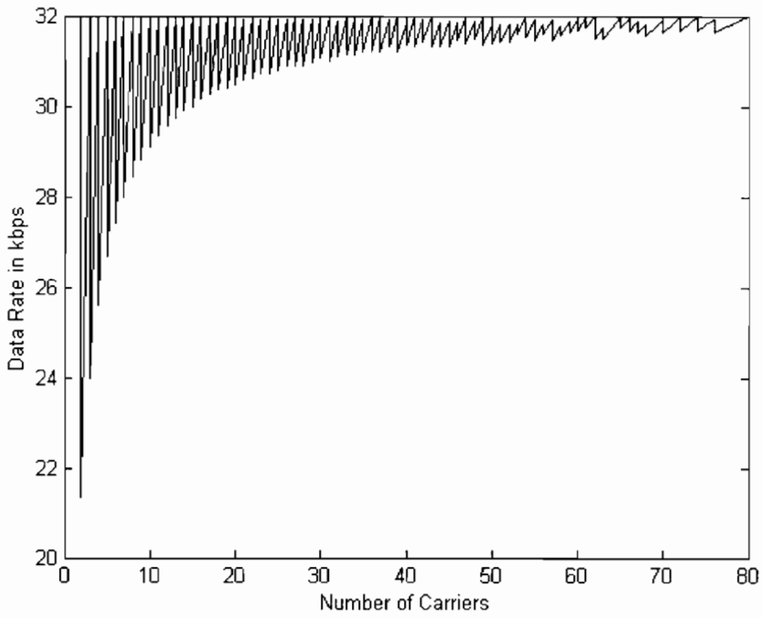

Figure 2.3: Data Rates vs. Number of Carriers (*N*)

In order to reduce the calculation time for the system it was decided to look at carrier values that were a power of 2, since most digital systems and algorithms are optimized for these values. The results are summarized in Table 2.1.

Number of Carriers	64	32	16
Data Rate	25.8560	25.9840	25.9840
Symbol Period	9.8 ms	4.9 ms	2.5 ms

Table 2.1: Data Rates and Symbol Periods for *N* a Power of 2

The results for $N = 32$ and $N = 16$ give slightly higher data rates, but the symbol periods are correspondingly shorter.

In order to make a final decision, the sample rate and the FFT length for the system had to be considered. A standard sample rate of 48000 samples/s was chosen. The FFT length should also be a power of 2 wherever possible in order to maximize the speed of the FFT. A value of 128 was chosen. Based on these values the smallest frequency that can be generated or detected by the FFT is:

$$f_{\min} = \frac{F_s}{N_{FFT}} \tag{2.3}$$

where F_s is the sample rate and N_{FFT} is the length of the FFT . Based on this the value for $f_{\min}$ is 375 Hz. This would give a maximum symbol period of 2.67 ms and a maximum number of carriers of 21. The number of carriers was reduced by 1 in order not to exceed the channel limits. The use of 20 carriers at a rate of 375 symbols/s with 4 bps, gives a final data rate of 30 kbps. The number of channels was therefore chosen to lie between 16 and 32 and gives a data rate close to the maximum of 32 kbps.

2.3 Initial Model Specification

The initial specification for the model is summarised in Table 2.2.

Available Bandwidth	8 kHz
Modulation Scheme	16-QAM
Bits per Symbol (bps)	4 bps
Sample Rate	48000 samples/s
FFT Length	128
No. of Carriers	20
Symbol Rate	375 symbols/s
Symbol Period	2.67 ms
Data-Rate	30 kbps

Table 2.2: Model Specification Summary

Chapter 3

Transmitter Simulation Model

This chapter deals with the implementation of the OFDM transmitter in the Simulink simulation environment. Simulink is a software package for modelling, simulating and analysing dynamic systems. The program was developed by The MathWorks. The package caters for continuous and discrete time models and hybrid models that are a mixture of the two [21].

3.1 Transmitter Overview

The basic transmitter block diagram is shown in Figure 3.1.

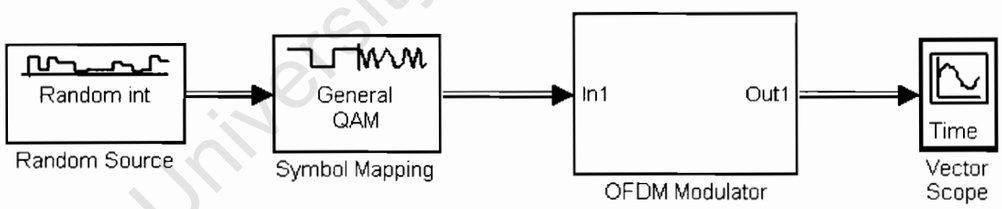

Figure 3.1: Basic OFDM Transmitter Model

The basic system consists of a data source, a symbol mapping block, an OFDM modulator and a simple sink (measurement or data block) in order to view the final waveforms. The data source generates random integer values and these values are

then converted to a baseband 16-QAM symbol by the general QAM block. The baseband QAM signal is then passed through to the OFDM modulator where an OFDM signal is generated using an IFFT block. The following sections will discuss the operation of the system in more detail.

3.2 Data Source and Mapping Blocks

3.2.1 Source

As was stated in the previous section the data source block is a random integer generator. This is in actual fact the same as a random bit generator combined with a bit-to-integer conversion block. The baseband QAM block accepts integer values in the range (0, M-1), therefore for a 16-QAM the integer generator would generate values between 0 and 15. This means that each of these integer values represents 4 binary digits or bits. The settings for the source block are shown in Figure 3.2.

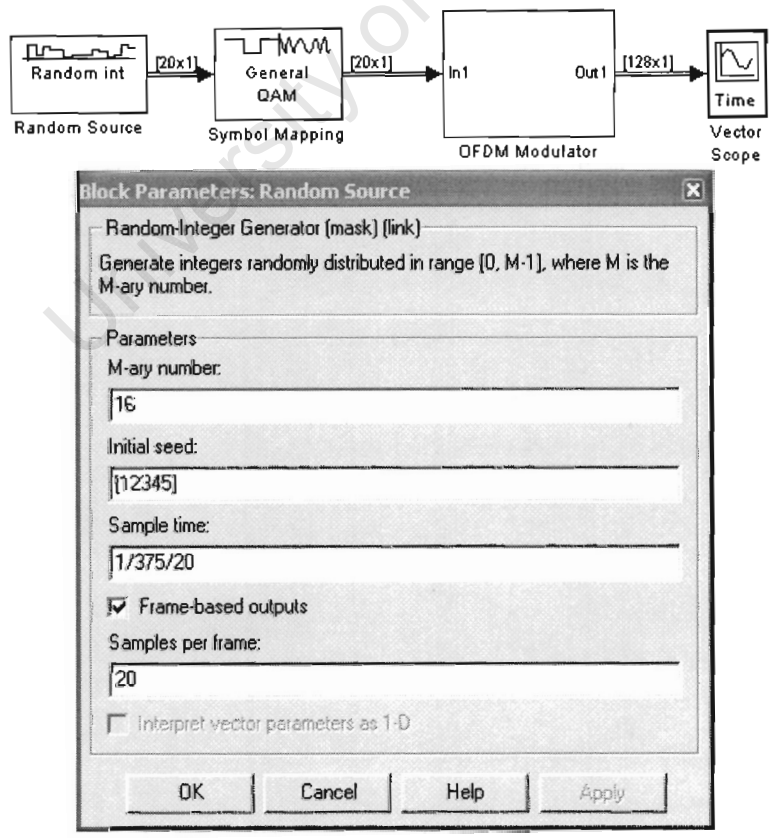

Figure 3.2: Settings for Random Source Block

The M-ary number is set to 16 since the chosen modulation scheme is 16-QAM. The initial seed has been left at its default setting. The output of the block is set to frame based. This means that the block will generate a 20x1 output vector of random integer values. Each value corresponds to the data for one of the sub-carriers in the system. The frame therefore represents the system data for one complete symbol. Since the frame will be passed on throughout the system, the sample time has to be set up at the source.

This sample time is not to be confused with the overall system sample rate, t_s = 1/48000 samples/s. This is the sample time required at the source in order to produce the required symbol rate, and hence required F_s, at the output of the OFDM modulator. The source sample time is given as $T_s = 1/f_{symbol}/N$. The values from the system specifications have been entered as shown in Figure 3.2.

3.2.2 General QAM Block

The QAM block takes the 20x1 vector from the source block and assigns each one of the integer values a corresponding complex value taken from a 16-QAM rectangular constellation. In other words the block maps the integer input to a 16-QAM complex baseband output. The constellation is a standard rectangular constellation given by the Matlab variable *qam_const_m16* and is shown in Figure 3.3.

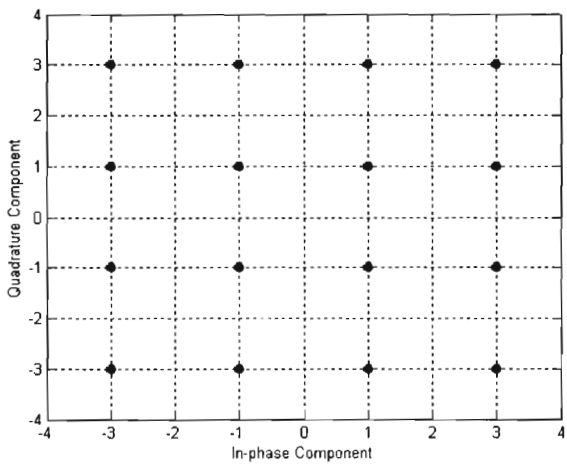

Figure 3.3: QAM Block Constellation

QAM mapping. The constellation has been set up using a Gray code, therefore the system source coding is conforming to the minimum coding requirements.

The settings for the QAM block are shown in Figure 3.4. Note that the "Samples per Symbol" field -is set to 1. The block must only output 1 QAM mapping per input. The frame rate for the output is thus the same as that of the input. If a binary input were used, the "Samples per Symbol" field would be set to 4 for a 16-QAM system.

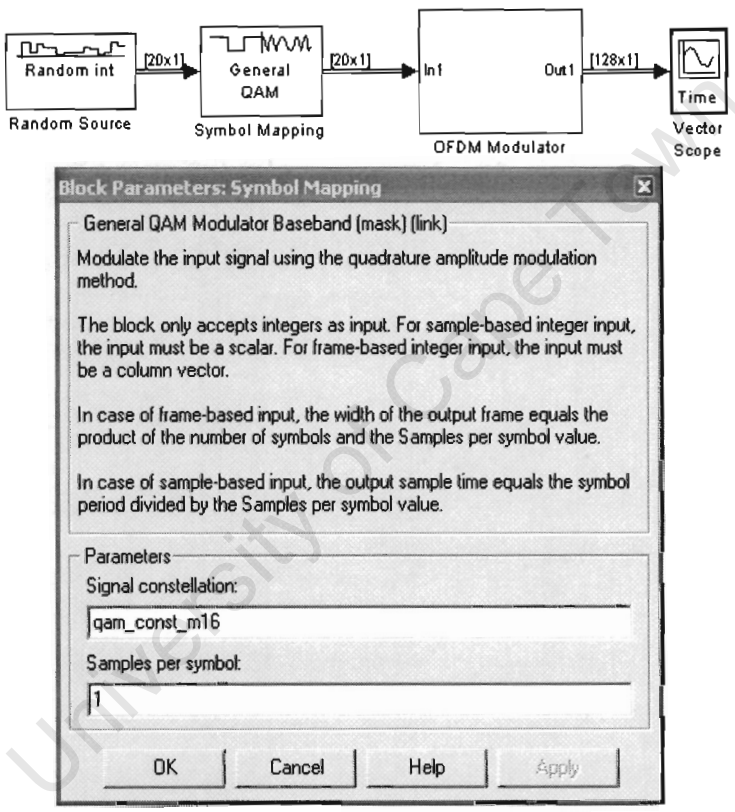

Figure 3.4:Settings for Symbol Mapping Block

3.3 The OFDM Modulator

In the block diagram of Figure 3.1, the OFDM modulator is shown as a single block. In actual fact it is made up of a number of smaller systems that have been combined to produce the desired result. Figure 3.5 shows the detailed view of the demodulator block.

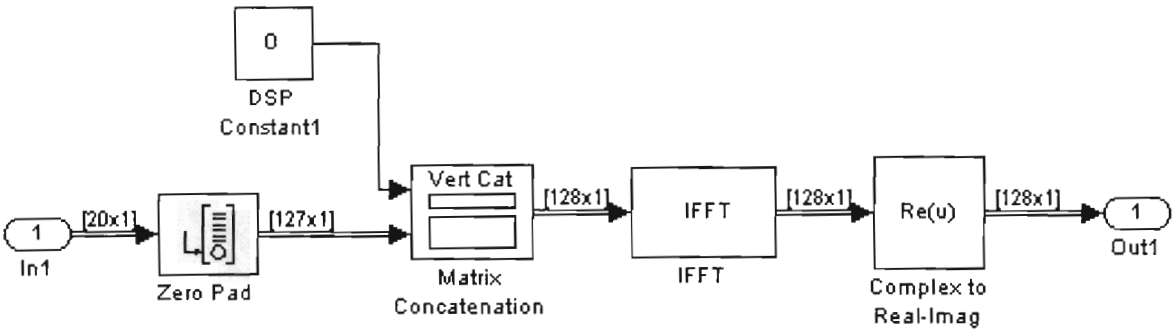

Figure 3.5: Detailed OFDM Modulator Block Diagram

The input to the OFDM block is the output from the QAM mapping block. This is a frame of data with dimensions 20×1. The FFT and IFFT blocks in Simulink only operate on vectors that have a length equal to a power of two. In order to increase the length of the input vector it has to go through a zero pad block.

The zero pad block will pad the input signal to a length of 127. It must be clearly noted at this point that the zero pad operation **preserves the frame rate**. The output of the zero pad block has the same output rate as the input, but it has more elements in the output vector. The zero pad operation therefore effectively increases the system sample time.

The 127×1 vector gets combined with a constant value of 0 to produce a 128×1 vector by concatenating the two inputs, the output from the zero pad block and a constant value of 0. The zero value is inserted so that the IFFT will not produce a signal with a dc offset. This new vector is then passed on to the IFFT block for further processing.

The output of the IFFT block is a complex signal that has been normalized by a factor of $1/N_{\text{IFFT}}$, where N_{IFFT} is the length of the IFFT. The reason why the output is complex is that the input data consists only of the complex valued symbols which have been zero padded to the correct length. If the matching complex conjugate symbol values had been included in the input data, then the output from the IFFT

would have been a real signal with zero imaginary values. The block implements the inverse FFT function as follows [22]:

$$x(n) = \frac{1}{N}\sum_{k=0}^{N-1} X(k) e^{j\left(\frac{2\pi}{N}\right)kn} \tag{3.1}$$

The imaginary part of the signal is removed by the Complex to Real-Imaginary block so that a real valued OFDM signal is generated. The output frame rate should be the same as the system symbol rate. A 3-frame output from the system is shown in Figure 3.6. The same frame was generated for consecutive symbol periods by limiting the M-ary value of the QAM block to 1. It can be seen that the symbols repeat approximately every 2.7 ms, which is the required symbol period for the system.

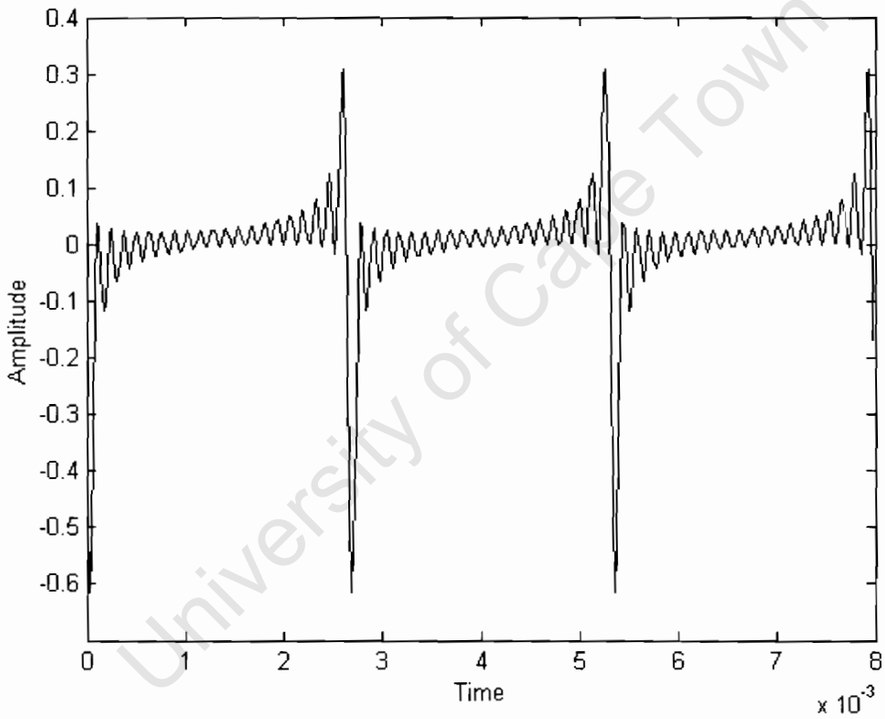

Figure 3.6: Output Signal from OFDM Transmitter Model

Chapter 4

Receiver Simulation Model

This chapter deals with the Simulink model for the OFDM receiver. The receiver essentially performs the reverse process that was performed at the transmitter. This section provides a general overview of the receiver model and a detailed discussion of the blocks used to implement the model in Simulink.

4.1 Receiver Overview

The receiver block diagram is shown in Figure 4.1.

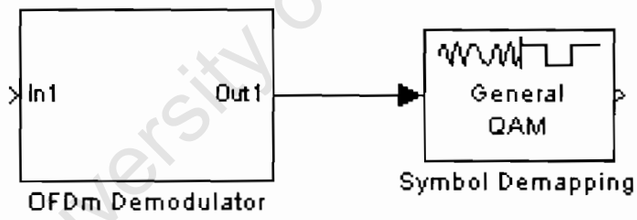

Figure 4.1: Basic OFDM Receiver Model

The basic system consists of the OFDM demodulator block and a general QAM baseband demodulator block. The basic operation is that the OFDM demodulator receives the OFDM signal from the transmitter, corrupted with noise, performs a FFT on the signal and outputs a vector of complex numbers that estimate one of the signaling points on the 16-QAM constellation. The Symbol Demapping block must

then make a decision as to which signaling point is closest to the estimated value in terms of magnitude and phase. Once this decision has been made a vector of integer values is then sent from the output of the block. These values can then be compared to the transmitted values in order to determine the symbol error rate (SER) or they can be converted to binary so that the bit error rate (BER) can be determined.

The fact that there are only two blocks in the receiver can be deceiving. The estimation and decision making process are the processes that make the largest computational demands on the system and require more complex algorithms than those used in the transmitter. The underlying process is hidden to a large degree from the user when using standard blocks such as the general QAM block.

4.2 Mathematical Background

Assume that the transmitted QAM signals are transmitted through a channel that introduces a carrier phase shift, and corrupts the signal with additive white Gaussian noise (AWGN). The transmitted signal for one sub-carrier in the system is given by [23]

$$s(t) = A_I g_T(t)\cos(2\pi f_c t) + A_Q g_T(t)\sin(2\pi f_c t) \tag{4.1}$$

where $g_T(t)$ is the pulse shaping function for the system.

Assuming that there is no appreciable attenuation through the channel, then the received signal will be

$$r(t) = A_I g_T(t)\cos(2\pi f_c t + \phi) + A_Q g_T(t)\sin(2\pi f_c t + \phi) + n(t) \tag{4.2}$$

where ϕ is the carrier phase shift and the AWGN component is

$$n(t) = n_I(t)\cos(2\pi f_c t) - n_Q(t)\sin(2\pi f_c t) \tag{4.3}$$

where n_I and n_Q are zero mean Gaussian random variables with the same rms values σ.

For detection, the received signal should be correlated with two synchronized basis functions in the receiver. These basis functions would ideally be

$$\psi_1(t) = A_I g_T(t)\cos(2\pi f_c t + \phi)$$
$$\psi_2(t) = A_Q g_T(t)\sin(2\pi f_c t + \phi) \quad (4.4)$$

The outputs from the correlators will be estimates of the amplitudes of the transmitted signals that have been corrupted by the noise in the channel and are given as

$$r_1 = A_I + n_I \cos\phi - n_Q \sin\phi$$
$$r_{12} = A_Q + n_I \sin\phi + n_Q \cos\phi \quad (4.5)$$

where the noise components are zero mean, uncorrelated Gaussian random variables with variance $N_0/2$.

These estimates are now passed on to a detector where the distance metrics (distance between the estimated signal point and all other points in the constellation) are calculated using the following

$$D(\mathbf{r}, \mathbf{s}_m) = |\mathbf{r} - \mathbf{s}_m|^2$$
$$\mathbf{r}^t = (r_1, r_2) \quad (4.6)$$
$$\mathbf{s}_m = \left(\sqrt{E_s} A_{Im}, \sqrt{E_s} A_{Qm}\right)$$

where m=1, 2,……., M and E_s is the energy in the transmitted signal.

4.3 The OFDM Demodulator

The internal construction of the OFDM receiver is shown in Figure 4.2.

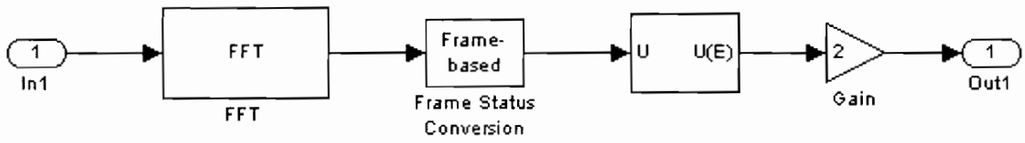

Figure 4.2: Detailed OFDM Demodulator Block Diagram

The input to the demodulator block comes directly from the channel model. The FFT block calculates the FFT of the received OFDM signal according to the formula [22]

$$X(k) = \sum_{n=0}^{N-1} x(n) e^{-j\left(\frac{2\pi}{N}\right)kn} \qquad (4.7)$$

The FFT block performs the correlation function mentioned in the previous section in order to produce the estimates required for the calculation of the metrics.

The output from the FFT block is a sample based signal and has to be converted back to a frame based one for further processing. This is the function of the Frame Status Conversion Block.

The purpose of the next block is to "re-order" the shape of the frame so that it can be applied to the QAM demapping block. The block parameter menu for the Selector block is shown in Figure 4.3.

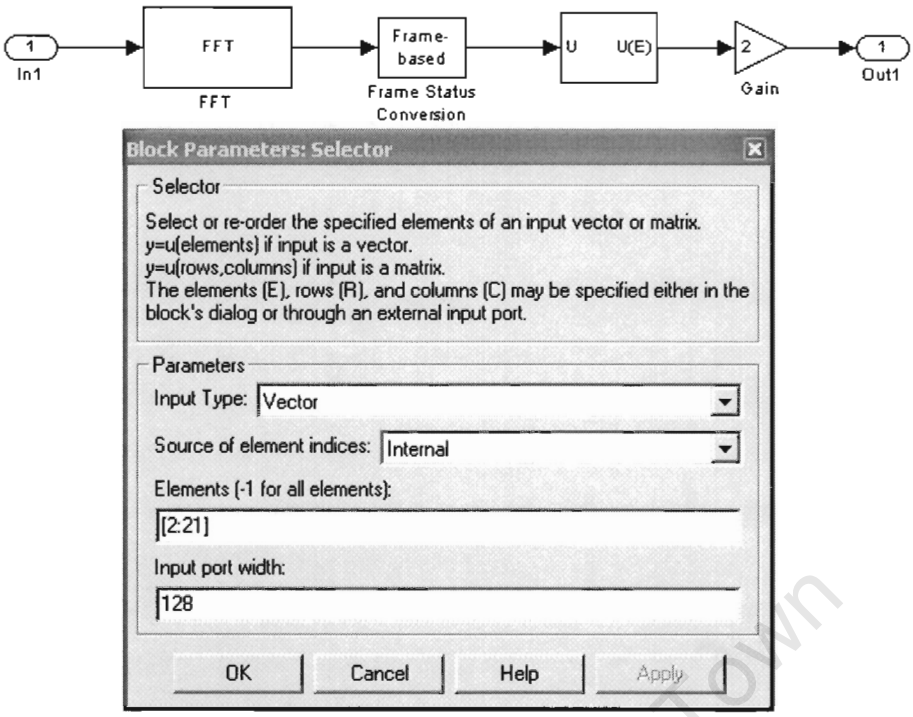

Figure 4.3: Selector Block Parameter Settings

Recall that in the transmitter, the output from the QAM mapping block had to be zero padded until it had a length equal to a power of 2. What the selector block does is reverse the process in that it removes the extra elements from the FFT block output so that only the relevant symbol information remains. The values of interest are the 20 FFT values that represent the data for the 20 OFDM carriers. These values are indexed from 2 to 21. In Matlab and Simulink the indices for arrays and vectors start at 1 and not 0. In this case the value at index 1 would represent a dc or average value, which is of no interest. The block therefore accepts a 128×1 vector input and passes a 20×1 vector output on to the next stage.

The gain block is required in the system since the selector takes only the 20 values from the FFT of interest. The FFT uses a complex exponential to calculate the output. The FFT vector includes values at the frequencies of interest and also complex conjugate values at the equivalent "negative" frequencies. The amplitude of the "positive" frequency and the "negative" frequency are both half the amplitude of the original (after normalization). If only one of the values is used, then it should be doubled in order to give the correct amplitude of the original signal. This is illustrated

by an example. The following array shows the values for a length 8 FFT for a fundamental cosine signal with an amplitude of 2. The sampling rate is 8 samples/s.

C1 =

Columns 1 through 4

-0.0000 8.0000 - 0.0000j 0.0000 -0.0000 - 0.0000j

Columns 5 through 8

0.0000 -0.0000 + 0.0000j 0.0000 8.0000 + 0.0000j

The conjugate column can be calculated in this case using a simple formula

$$Conjugate\ index = (N_{FFT} + 2) - Current\ Index$$

If the current index is 2 then the conjugate is located at index 8. The selector block would only take the value at index 2 since this corresponds to the amplitude of the first sub-carrier. After normalization by the length of the FFT this would leave a value of 1 for the amplitude. In order to correct this a scaling factor of 2 has to be introduced into the system.

The original signals have been corrupted with noise, may have undergone a certain amount of attenuation and may have experienced a carrier phase shift. The output frame from the OFDM demodulator therefore contains estimates of the original signal amplitudes and phases that were sent from the transmitter. It is the task of the demapping block to make a decision as to what these original amplitudes and phases were, based on the estimates received from the OFDM demodulator.

4.4 The Symbol Demapper

The demapping block is simply the detector mentioned in Section 4.2. The demapping block must accept the estimate from the correlator, in this case the OFDM demodulator block, and determine which of the original signal constellation points were transmitted. The process is illustrated graphically in Figure 4.4.

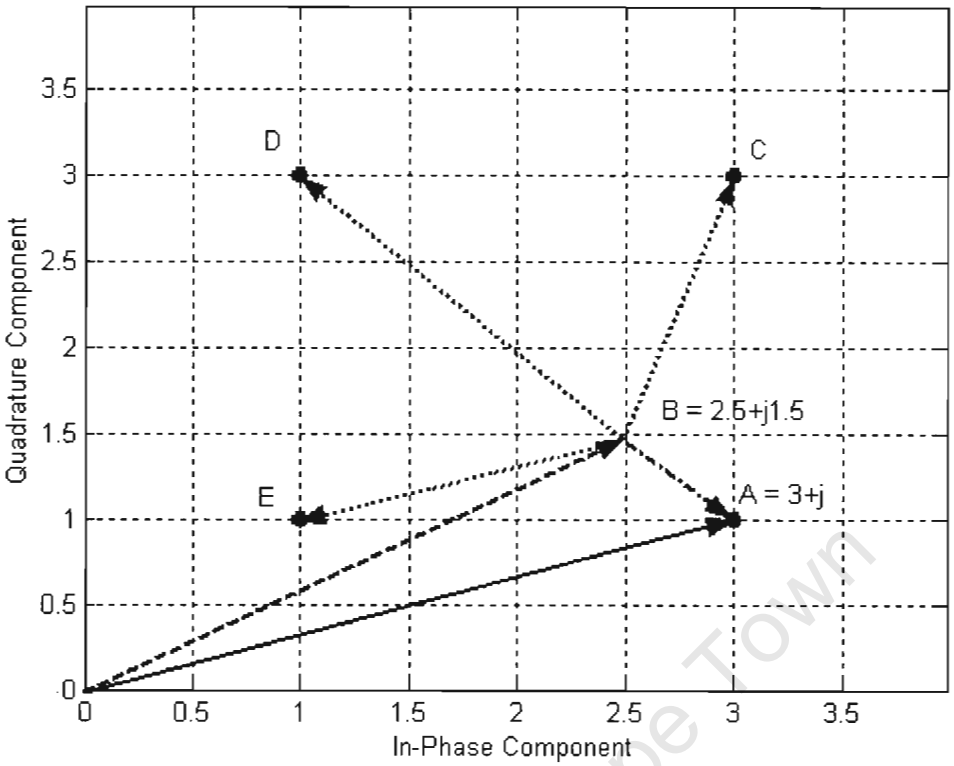

Figure 4.4: Graphical Illustration of the Demapping Process

In Figure 4.4 only one quadrant of the 16-QAM constellation is shown. Assume that point A = 3+j was the original signal point transmitted. Due to noise etc in the channel the OFDM demodulator estimates the value of the received signal to be 2.5+j1.5 (point B). The QAM demapping block must decide which of the constellation points the estimate is most likely to represent. In this case it would calculate the metrics between the estimated signal point and the actual signal points. These metrics are shown by the dotted line. The signal point that gives the shortest metric is chosen as being the transmitted point in the constellation. Only 4 possibilities are shown in Figure 4.4, for a 16-QAM system there are 16 possibilities that have to be considered. Some systems limit the metric calculation to a single quadrant.

This whole process is represented by a single Simulink block. This tends to make the receiver appear to be rather simple, but knowledge of the underlying process is required for the proper understanding of the system operation.

Chapter 5

Channel Simulation Model

Chapter 5 deals with the modelling of a suitable channel for use in the system simulation. The channel model is based on measurements taken from an Agilent Technologies HP8920A Radio Frequency Communications Test Set. A block diagram of the test setup and the measurements are given in Appendix B.

5.1 Background

In general communications channels can introduce a number of unwanted parameters into the transmitted signal such as noise, fading and other interference [24]. In general the channel model is based on a mathematical description of the channel. If a mathematical expression is not readily available, then measured results can be used to approximate channel behavior.

The packet radio environment makes use of FM tranceivers to transmit and receive information. The Simulink Communications Blockset has a passband FM Modulator block and a corresponding FM demodulator block. Since the FM blocks work on carriers, the effect of introducing these blocks into the simulation models is that the overall sample rates for the system have to increase to accommodate the higher carrier frequencies. This tends to put extra computational loading on the system.

If investigations are not specifically aimed at the behaviour of the transmitted and received high frequency carriers then the modulation and demodulation components

can be included in the channel model. This has the advantage that no high frequency signals are present in the simulation. The FM demodulator block uses a voltage controlled oscillator and a low pass filter to model the demodulation process. The approach for the modelling of the proposed channel is to physically measure the input and output signals to the FM tranceiver and model the whole system using an appropriate filter transfer function.

5.2 The Measured Channel

Figure 5.1 shows a graph of the actual measured response for the HP8920A Test Set. A table of measured values is given in Appendix B. The carrier frequency was set to 145 MHz with an output power of –20 dBm. No pre- or de-emphasis was employed.

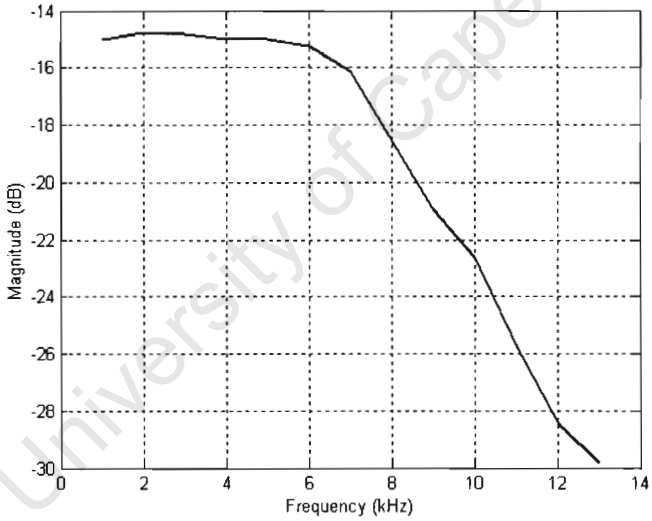

Figure 5.1: Measured Frequency Response of HP8920A

The group delay in samples (sampling rate 48000 samples/s) for the system is shown in Figure 5.2. The values shown are calculated by

$$n_{\text{delay}} = T_{\text{delay}} f_{\text{samp}} \qquad (5.1)$$

where n_{delay} is the delay in samples, T_{delay} is the measured delay of the system and f_{samp} is the sampling rate used for the simulation model. This delay was used to initially determine the type of filter used as will be discussed in the next section.

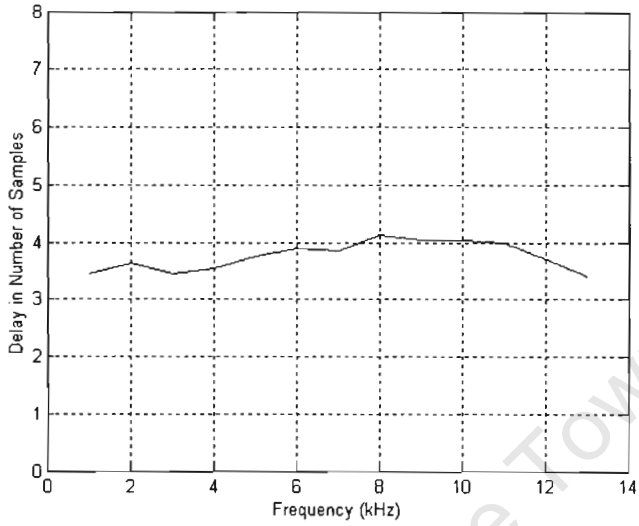

Figure 5.2: Equivalent Sample Delay

5.3 Modeling the Channel Using the FDA Tool

Simulinks Filter Design and Analysis tool was used for the design of the channel model. The filter was designed using the Arbitrary Amplitude option in the FDATool GUI. The arbitrary amplitude option makes use of the Remez exchange algorithm and reduces the minimax (or Chebyshev) filter error to produce equiripple FIR filters. A full discussion of the function is given in the Simulink Help files.

A finite impulse response (FIR) filter was chosen because of the group delay of the measured channel. It was approximately constant over the frequency band of interest as is shown in Figure 5.2. This would indicate that the filter has linear phase characteristics and suggested the use of a FIR filter. The magnitude of this delay was approximately 4 samples. This translates to an eighth order filter since the delay for a linear phase FIR filter is half of the filter order.

The template for the filter design is shown in Figure 5.3.

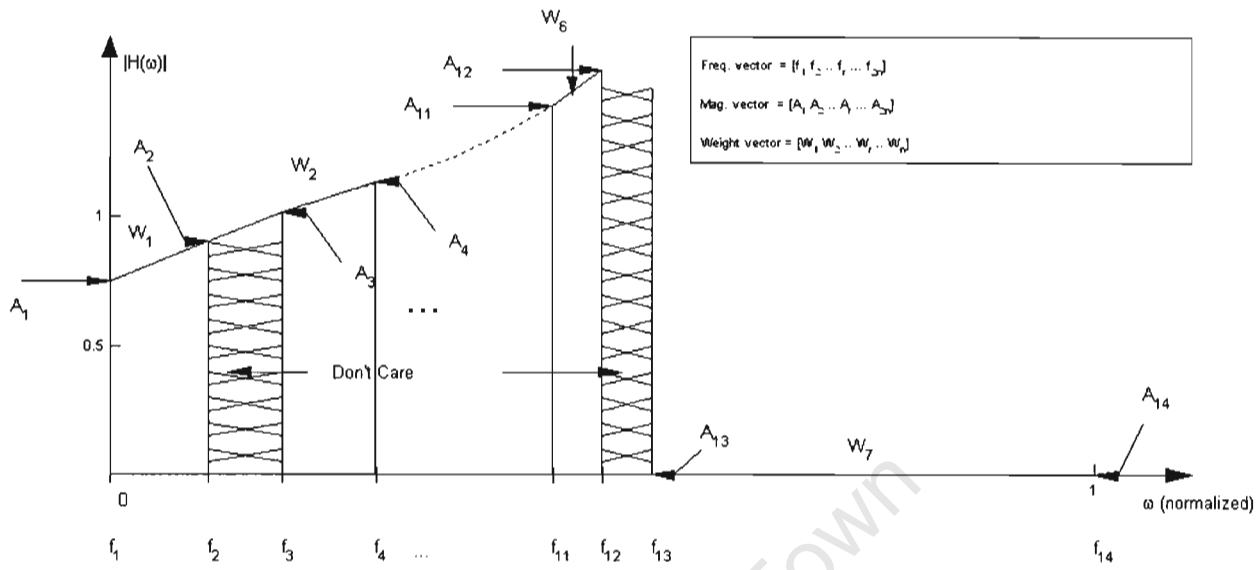

Figure 5.3: FDATool Template for Arbitrary Magnitude Filter Design

The explanation of the template is taken directly from the Simulink Help files. The designer has to specify an array of normalised frequencies that will be used in the design. These frequencies are specified in the range between 0 and 1, where 1 corresponds to the Nyquist frequency. The frequencies must be in increasing order. These values are given in the frequency vector **f**. Another vector, **a**, specifies the magnitude characteristics of the filter. Vectors **f** and **a** must have the same length and must be even. The desired amplitude at frequencies between pairs of points (**f**(k), **f**(k+1)) for k odd is the line segment connecting the points (**f**(k), **a**(k)) and (**f**(k+1), **a**(k+1)). The desired amplitude at frequencies between pairs of points (**f**(k), **f**(k+1)) for k even is unspecified. The areas between such points are transition or "don't care" regions. A third vector, **w**, must also be specified. This vector specifies the "weightings" that will be used to fit the response curve in each of the frequency bands. The length of **w** must be half the length of **f** and **a**.

The original measured frequency response was modified to include a number of 100 Hz "don't care" values between each of the frequencies of interest. The modified response is shown in Figure 5.4.

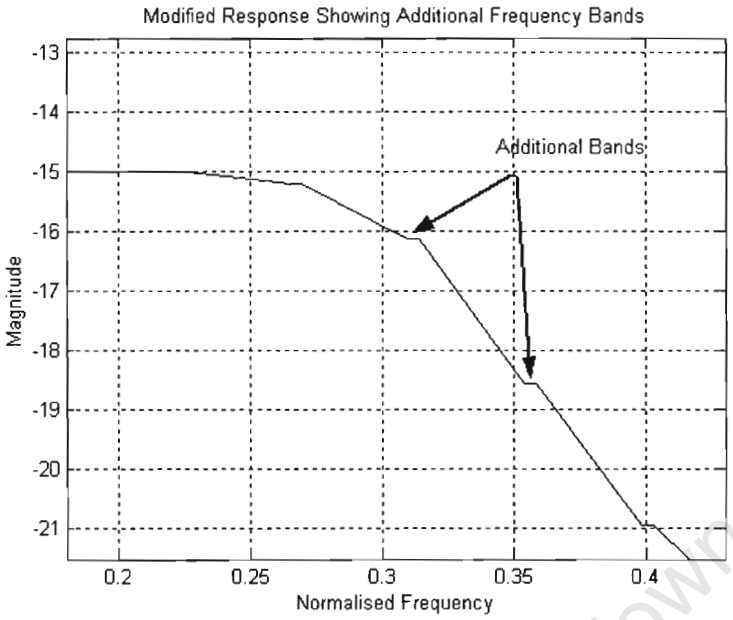

Figure 5.4 Modified Channel Response with Additional "Don't Care" Bands

The final parameters for the filter design are shown in Table 5.1:

Parameter	Value
Sampling Rate	48000 samples/s
Filter Type	Arbitrary Magnitude
Design Method	Equiripple FIR
Order	8
Frequency Units	Normalised
Weighting Factors	Default
Frequency Vector	norm_freq_vect48
Magnitude Vector	norm_mag_vect
Weighting Vector	[10*ones(1,16) 10]

Table 5.1: Final Filter Design Parameters

The filter was designed using the FDATool and the coefficients exported to Matlab. Making use of the *freqz.m* m-file, the designed filter response is compared to the measured channel response in Figure 5.5. The measured response is shown by the

solid line, and the modelled response by the dash-dot line. The extended dash-dot line in the figure is the first side-lobe of the FIR filter.

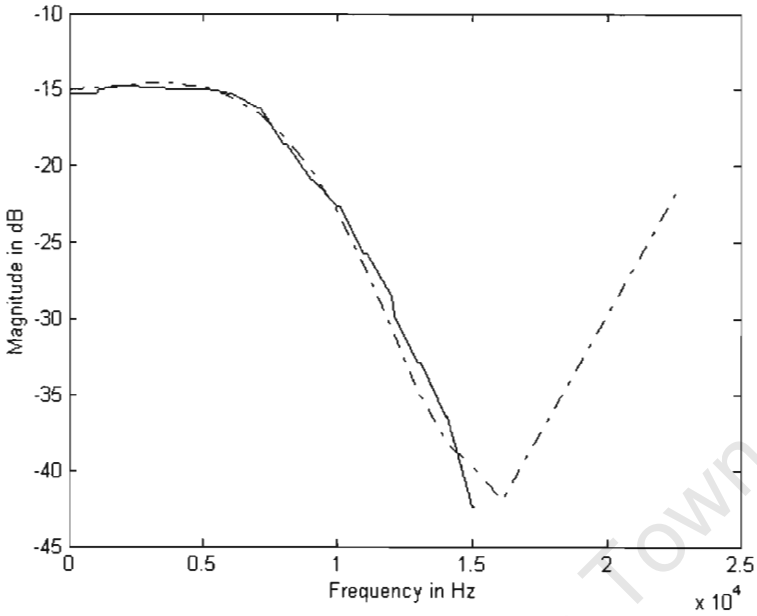

Figure 5.5 Comparison of Design Response to Measured Response

It must be noted at this point that the model chosen was the simplest one for this channel. In practise the channel would fade and produce variations in group delay at different frequencies. The simple model does not simulate fading, and has a constant group delay. The model however was sufficient for the evaluation of the proposed OFDM system.

5.4 Noise in FM Systems

A detailed analysis of the noise in angle-modulated systems can be obtained in [25][26]. It is often convenient to express the noise in FM systems in terms of its envelope and phase as

$$n(t) = r(t)\cos\left[2\pi f_c t + \psi(t)\right] \qquad (5.2)$$

where the envelope and phase can be defined in terms of the in-phase and quadrature components as

$$r(t) = \sqrt{n_I^2(t) + n_Q^2(t)}$$
$$\psi(t) = \tan^{-1}\left(\frac{n_Q(t)}{n_I(t)}\right) \tag{5.3}$$

If the signal at the output of the IF filter is given by

$$s(t) = A_c \cos\left[2\pi f_c t + \phi(t)\right] \tag{5.4}$$

where

$$\phi(t) = 2\pi k_f + \int_0^t m(t)dt \tag{5.5}$$

then the total signal plus noise at the output of the IF section is

$$s(t) = A_c \cos\left[2\pi f_c t + \phi(t)\right] + r(t)\cos\left[2\pi f_c t + \psi(t)\right] \tag{5.6}$$

It can be shown [26] that under the conditions of high carrier-to-noise ratio, the calculations for the average output noise power in an FM receiver depend only on the carrier amplitude, A_c, and the quadrature noise component, $n_Q(t)$. Therefore the equation for the output noise is given as

$$\text{Average power of output noise} = \frac{2N_0W^3}{3A_c^2} \tag{5.7}$$

For the parameters on which the model was based, carrier power –20 dBm and $W = 8$ kHz, (5.7) gives the average power of output noise as 137 μW.

5.5 Implementation Using Simulink

The Simulink model for the channel is shown in Figure 5.6.

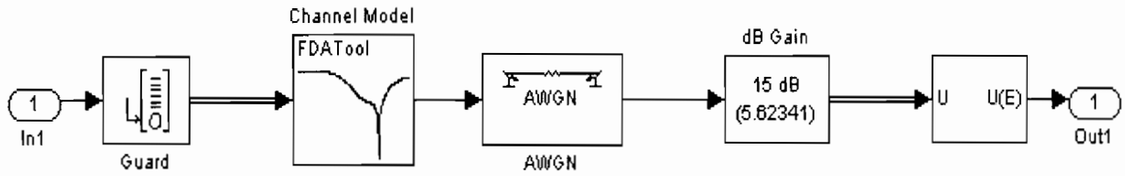

Figure 5.6: Simulink Channel Model

The components that actually model the channel are the channel model filter, and the AWGN block. The AWGN block is used to generate a Gaussian random noise signal that is added to the real OFDM output signal from the channel filter. Details of the channel filter have been discussed at length in the section.5.3. A 15 dB gain block was inserted to compensate for the attenuation introduced by the channel filter.

The guard block appends a simple 4-sample guard band to the OFDM signal. The guard band is removed by the selector block at the end of the Simulink model. The guard band in this case is used to compensate for the resultant delay introduced into the transmitted symbol rather than to reduce any intersymbol interference. The resultant symbol period increases from 2.67 ms to 2.75 ms, and the system data rate drops from 30000 bps to 29040 bps.

Chapter 6

Peak-to-average Power Ratio

Peak-to-Average Power Ratio (PAPR) is a problem in multi-tone systems since there is a potential to drive the transmitting amplifiers into saturation thereby causing non-linear distortions that cannot be corrected in the receiver. This chapter briefly discusses some of the techniques available to combat PAPR. The chapter will end with a brief discussion on A-Law companding which has been proposed by Wang for the reduction of PAPR [27].

6.1 Overview

The applications for OFDM systems have increased over the last decade. In many systems there are a large number of carriers, 256 in an ADSL system for example. If the carriers have equal amplitude, the potential worst case PAPR is given by $10\log_{10}(N)$ dB where N is the number of sub-carriers in the system. In the case of the system presented the number of sub-carriers is 20 which leads to a PAPR of 13 dB. The presence of these peaks require increased design complexity such as high resolution D/A-/D converters and line drivers that exhibit linear behavior over a large dynamic range [18]. If the amplifiers are driven into their non-linear region, saturation can occur and intermodulation distortion is introduced into the transmitted signal. One way to combat this is to use "power back-off"[28], where the power in the transmitted signal is reduced so that the amplifier operates in its linear region. For high PAPR this

"back-off" could be considerable, leading to inefficient use of the system. The next section will discuss a number of methods that are used to reduce PAPR.

6.2 PAPR Reduction Techniques

6.2.1 Clipping

With the clipping option, the designer allows for the occasional saturation of the power amplifiers. The problem with clipping is that it can introduce non-linear signal components that are difficult, if not impossible, to compensate for at the receiver. A number of publications have been published that discuss signal degradation due to clipping in OFDM systems [29]. Clipping reduces the PAPR and improves efficiency, but it introduces clipping noise.

6.2.2 Phasing

One way to reduce PAPR is to make sure that the carriers do not all have the same magnitude at the same time. One way to prevent this is to change the phase shifts between the various carriers. These phase shifts can be selected pseudorandomly or they can be generated by algorithms, or by the use of different codes. There have been numerous investigations into this type of reduction technique. To show a few examples, [30] makes use of coding and phasing while [31] makes use of trellis shaping, which was originally used to minimize the average transmitted power in single-carrier systems. Many of the proposed techniques require significant coding overhead an add complexity to the transmitter. As a result, clipping is still a widely adopted reduction technique.

6.2.3 Companding

There are two types of companding systems that are in widespread use today, namely mu-law and A-law companding. A-law companding is used in Europe while mu-law companding is used in the United States and Japan. Companding is basically the

process whereby a signal is *compressed* and then *expanded*. In a companded system, higher amplitude signals are amplified less than lower amplitude signals. The overall effect is that the higher amplitude signals appear to have been compressed when compared to the companded signal. The reverse process takes place at the receiver. Wang, *et al*,[27] proposed the use of an A-law compander for use in OFDM systems.

The compression characteristic for A-law companding is [32]

$$V_{out} = V_{\max}\left(\frac{A\frac{V_{in}}{V_{\max}}}{1+\ln A}\right) \qquad 0 \le \frac{V_{in}}{V_{\max}} \le \frac{1}{A} \qquad (6.1)$$

$$V_{out} = V_{\max}\left(\frac{1+\ln\left(A\frac{V_{in}}{V_{\max}}\right)}{1+\ln A}\right) \qquad \frac{1}{A} \le \frac{V_{in}}{V_{\max}} \le A \qquad (6.2)$$

Parameters to be specified are A (compression factor with a default of 87.6) and Vmax (maximum uncompressed input amplitude). The proposed system will use A = 16 based on the recommendations in [27]. Figures 6.1 and 6.2 show the curves for the A-law compander using (6.1) and (6.2) and compare the compression factor of A = 16 to the default value of A = 87.6.

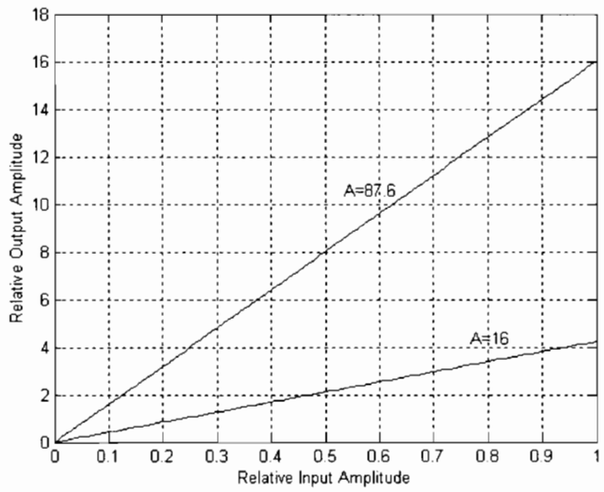

Figure 6.1: Comparison of Compression Factor Using Equation (6.1)

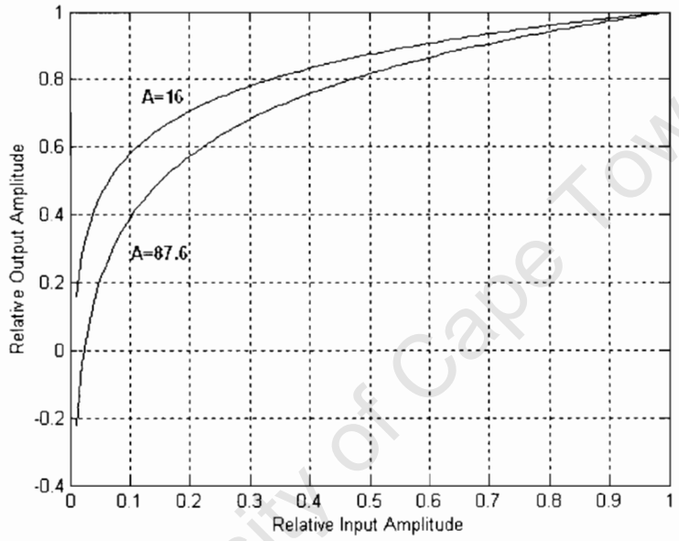

Figure 6.2: Comparison of Compression Factor Using Equation (6.2)

Figure 6.1 shows that over the range $0 \le \frac{V_{in}}{V_{\max}} \le \frac{1}{A}$, a system with a higher compression factor will give greater amplification to smaller input amplitudes. This would make sense as the "compression" actually takes place by increasing the amplitude of the low amplitude signals relative to the higher amplitude signals.

Over the interval $\frac{1}{A} \le \frac{V_{in}}{V_{\max}} \le A$, the higher compression factor provides less amplification to the high amplitude signals as can be seen in Figure 6.2. The

difference in the amplification is less pronounced than at the lower amplitude levels. It is interesting to note that the A-law function exhibits a linear characteristic over the interval $0 \le \frac{V_{in}}{V_{\max}} \le \frac{1}{A}$.

6.3 Companding Systems in Simulink

The Simulink Communications Blockset contains standard A-law compression and expansion blocks in its source coding library. Figure 6.3 shows a basic A-law companding system.

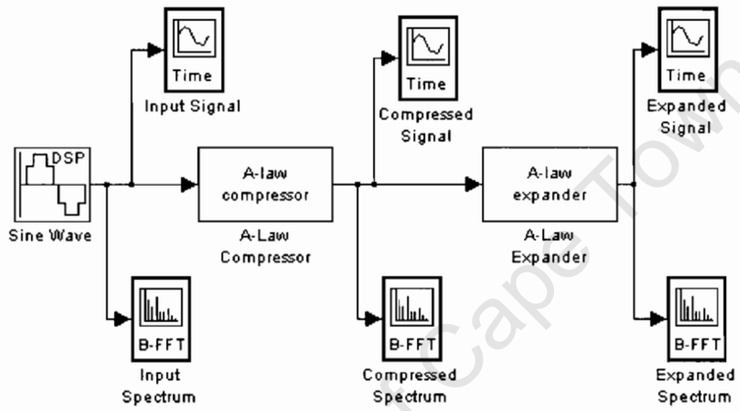

Figure 6.3: A basic A-law Companding System

The system consists of a simple sinewave generator that produces a 100 Hz sinusoidal waveform. The A-law compressor and expander have been given the parameters that A = 16 and V_{max} = 0.8V. The frequency spectra for the system are shown in the following figures:

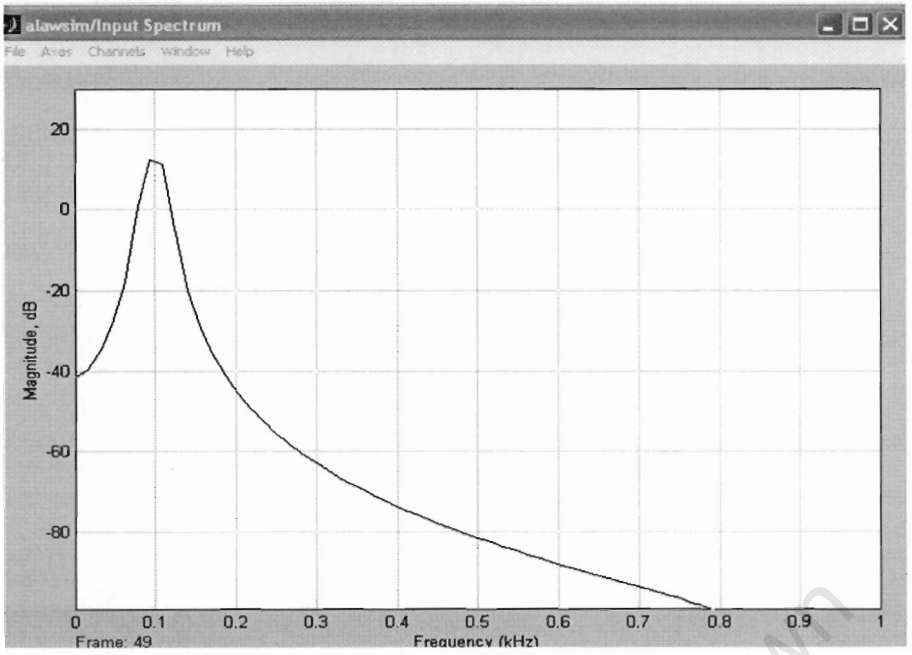

Figure 6.4: A-law Compressor Input Spectrum

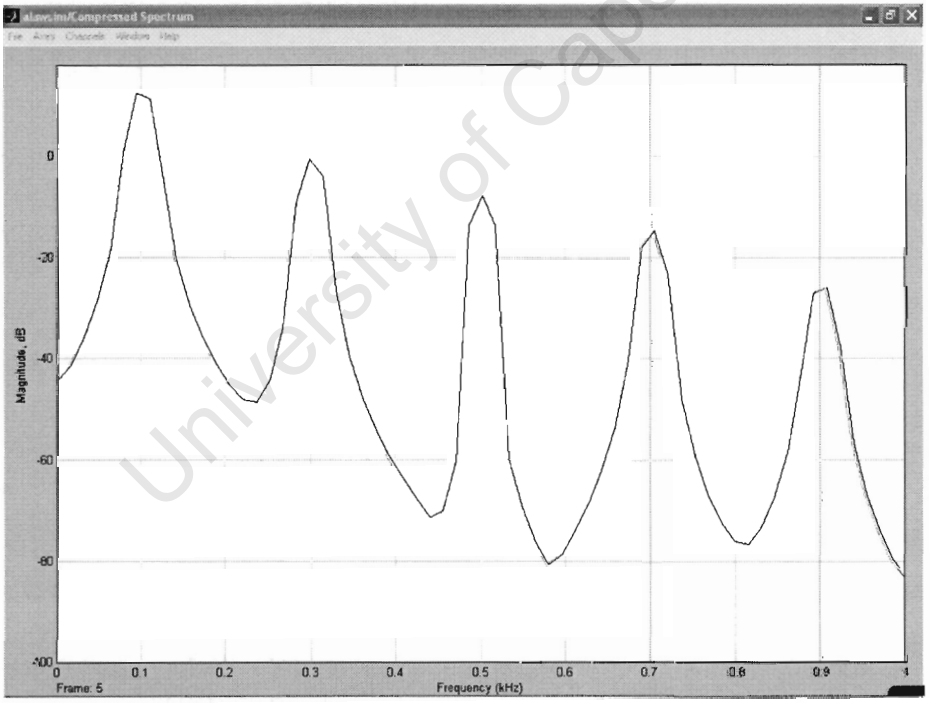

Figure 6.5: Compressed Signal Spectrum

Figure 6.4 shows the frequency spectrum of the input signal. A spectral peak can be seen at 0.1 kHz as expected. Figure 6.5 shows the spectrum of the compressed signal. It can be seen that the compression process introduces a number of odd harmonics into the compressed signal. The introduction of these harmonics has the effect of

making the compressed signal look more like a square waveform. One could view the compression process as something that keeps the zero crossings of the sinusoidal waveform fixed in order to preserve the time information and then push the signal peaks towards the required compression level. This "squaring up" of the waveform becomes more pronounced as more compression is required. This is illustrated in Figure 6.7, where V_{max} is reduced from 0.8 V to 0.4 V.

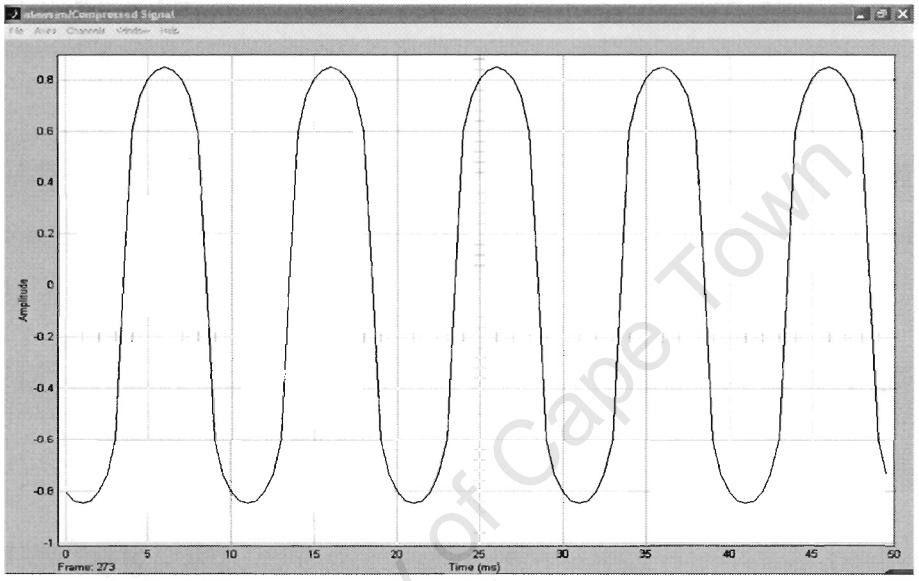

Figure 6.6: Compressed Signal

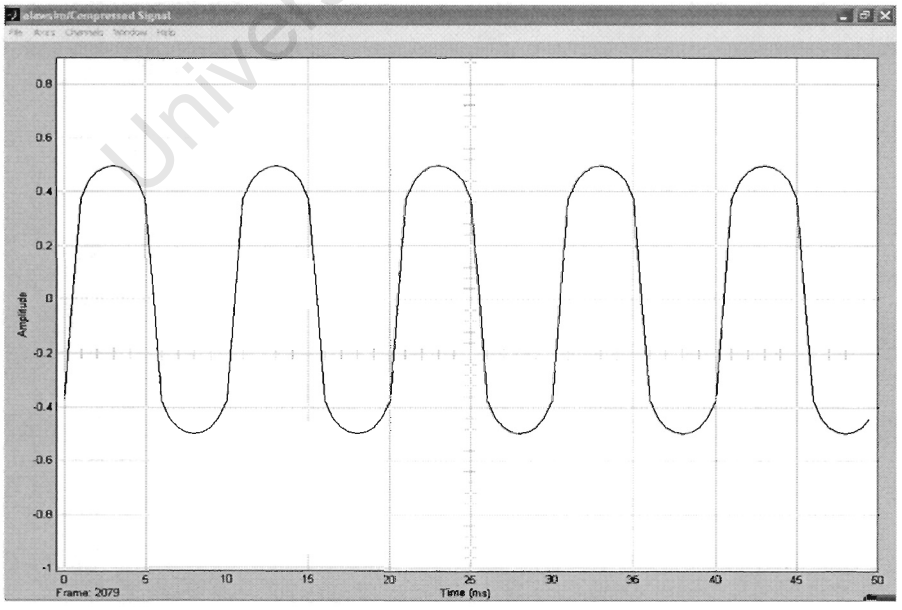

Figure 6.7: Compressed Signal With V_{max} = 0.4 V

This generation of odd harmonics has implications for the use of the A-law compressor in OFDM systems, especially when the transmission medium has a limited bandwidth. This will be discussed in Chapter 7 when considering the simulation results.

Chapter 7

Simulations and System Performance

The simulation results of the models developed in the previous chapters will be discussed. The theoretical error rate for 16-QAM will be covered and used as a benchmark to measure the performance of the rest of the system. The basic OFDM model symbol error rate (SER) will be investigated with and without the channel model. Simulations using a companded system will be used to evaluate system performance with and without the channel model and also with and without the presence of AWGN.

7.1 Theoretical 16-QAM SER

The discussion in this section is based on reference [23] and the 16-QAM system developed in Chapter 7.4 of that reference will be used as a basis for the performance comparisons in this chapter.

If an optimum detector is used that bases its decisions on the optimum metrics discussed in Chapter 4, then it can be shown that the upper bound on symbol error probability for a M-ary QAM system is given by

$$P_M \leq 4Q\left(\sqrt{\frac{3k\mathrm{E}_{avb}}{N_0(M-1)}}\right) \qquad (7.1)$$

for any k=1, where E_{avb}/N_0 is the average signal-to-noise (SNR) per bit., $M=2^k$ and $Q(k)$ is the complementary error function [23]. The error probability is plotted in Figure 7.1 as a function of the average SNR per bit for various M-ary systems. The Matlab code for these plots can be found in Appendix A.

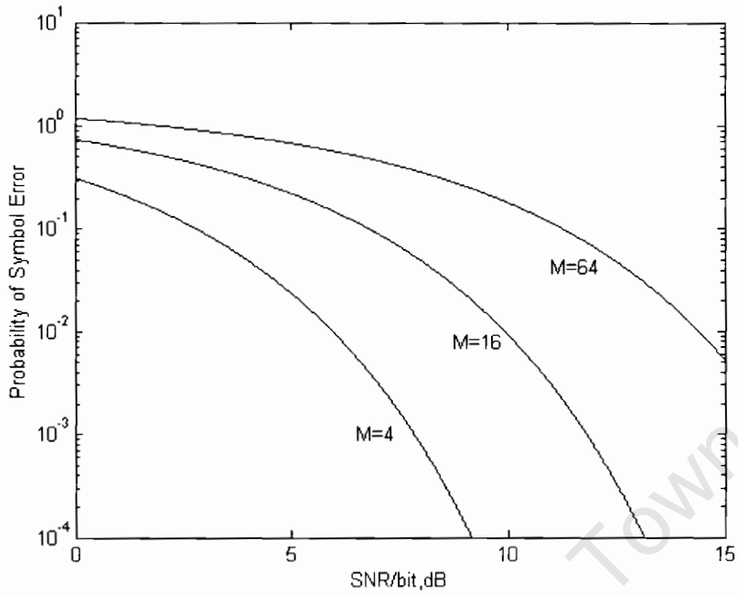

Figure 7.1: Theoretical Symbol Error Probability

The theoretical symbol error probability shown will be used to evaluate the performance of the developed simulation models.

7.2 OFDM Model with Single and Multi-Carriers, No Channel

This simulation is to check the operation of the system with a single carrier where there would be no inter-carrier interference in the model, and compare the result to the theoretical error probability. No channel is used because the performance of the transmitter and receiver models is being checked. The simulation model for this section is shown in Figure 7.2.

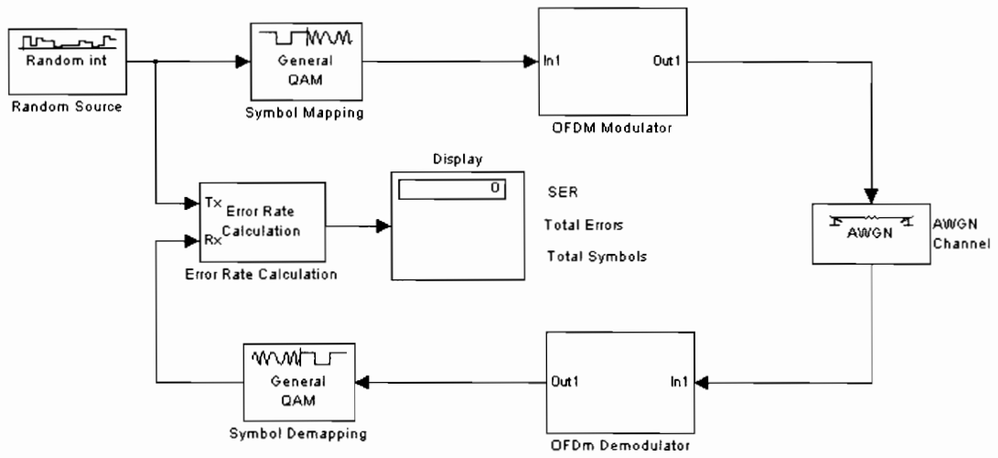

Figure 7.2: Basic OFDM Simulation Model, No Channel

The results for the simulation are shown graphically in Figure 7.3.

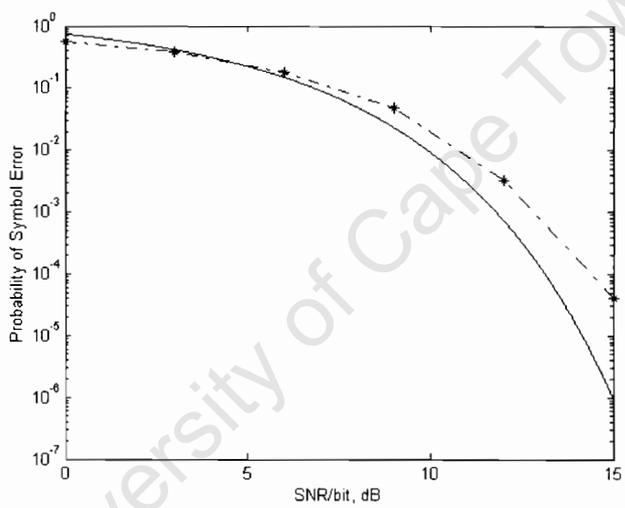

Figure 7.3: Probability of Error for a Single Carrier

Figure 7.3 shows that the model is performing close to the theoretical bound. The graph indicates that the system model does not reach the best possible probability of error at higher signal to noise ratios. This must be kept in mind when analysing later models. The results of the simulation using 20 carriers were almost identical thus showing that the basic model is not introducing any excessive noise or distortion into the OFDM multi-channel model.

7.3 OFDM Model with Companding , No Channel

In Chapter 6 the use of companding techniques were discussed for the reduction of PAPR. This section makes use of the A-law compressor and expander blocks in Simulink to determine the performance of the modelled OFDM system using companders. The simulation model for this section is given in Figure 7.4.

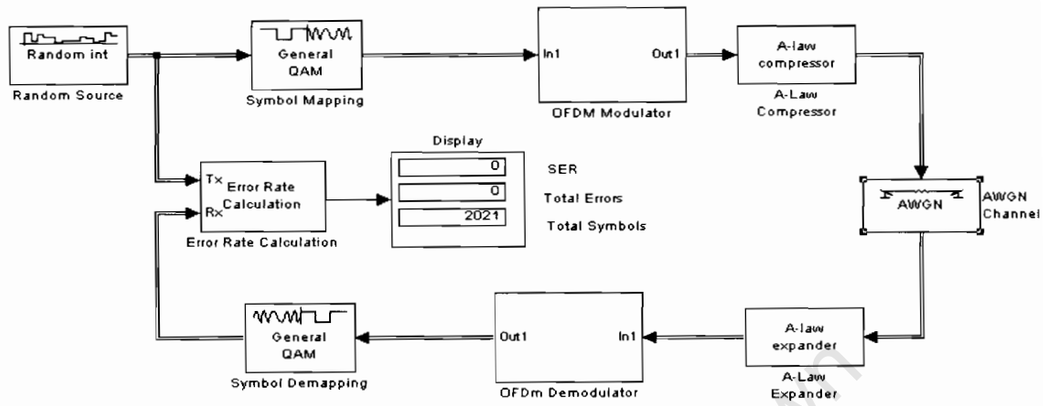

Figure 7.4: Basic OFDM Companding SER Simulation

The results of the simulation for a single carrier and 20 carriers are shown in Figure 7.5.

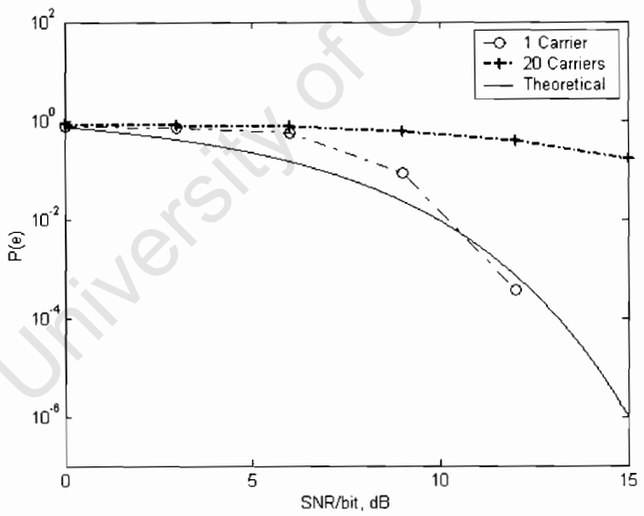

Figure 7.5: SER for Companded Model

The results for the single carrier system show that the SER for a single companded carrier only start to approach the theoretical values at about 10 dB. For the 20-channel

system the SER performance is rather poor. In chapter 6 it was shown the compression of a signal generated odd harmonics. Since the carriers in the system are harmonically related the odd harmonics generated in the compression process would result in inter carrier interference. This is a problem would occur even at high values of SNR which would account for the poor performance shown by the 20-carrier system even when low values of noise are present. This situation would be made worse if a high degree of compression were required.

7.4 OFDM with Channel and AWGN

Figure 7.6 shows the model used for the final Simulation. This system comprises of the modelled transmitter, receiver and channel model.

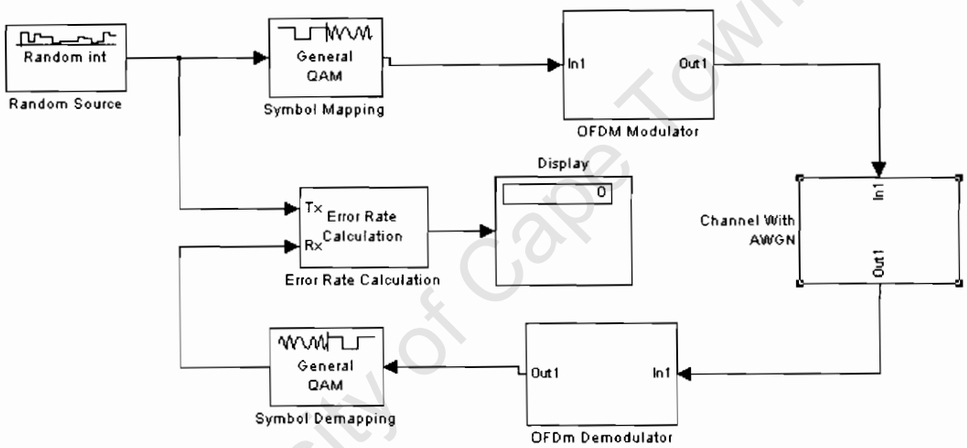

Figure 7.6: Full OFDM System Model

The internal structure of the channel model is shown in Figure 7.7.

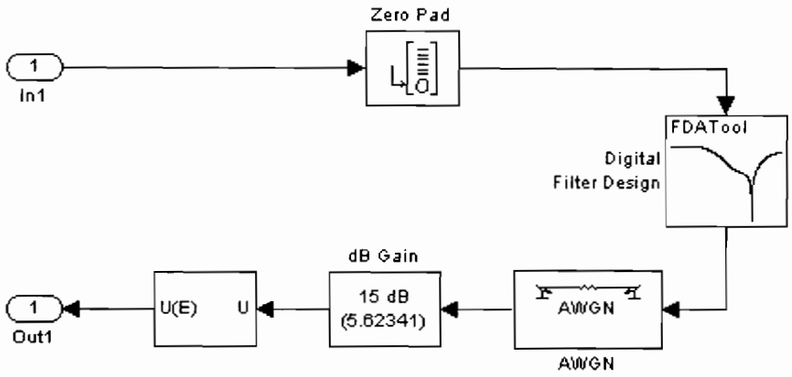

Figure 7.7: Internal Structure of the Channel Model

The results of running the error simulations is shown in figure 7.8 for both single and multi-carrier systems.

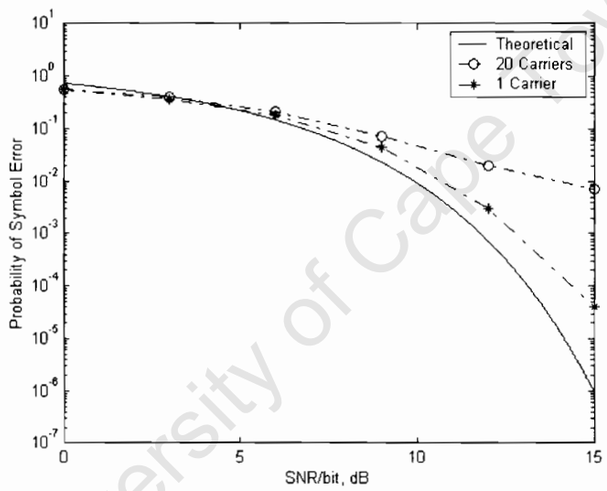

Figure 7.8: Error Simulation Results for OFDM System with Channel and AWGN

Comparing Figure 7.8 to Figure 7.3 it can be seen that the single carrier OFDM performed much the same with the channel and AWGN as it did with just the AWGN. The 20-carrier system did not perform as well as can be seen from Figure 7.8. From the data in Appendix C, the error rate for the 20-carrier system at 15 dB SNR was 0.00731. The system would be expected a far better error rate, closer to 0.0007, at such a SNR.

In order to improve the probability of error, the number of sub-carriers was reduced. Table 7.1 shows a comparison of a 16-channel system and a single channel system. These results are shown graphically in Figure 7.9.

SER, dB	1 Carrier SER	16 Carrier SER
0	0.5532	0.5499
3	0.3727	0.3709
6	0.1775	0.1784
9	0.04546	0.04576
12	0.003	0.00445
15	4e-05	6e-05

Table 7.1: Comparison of SER

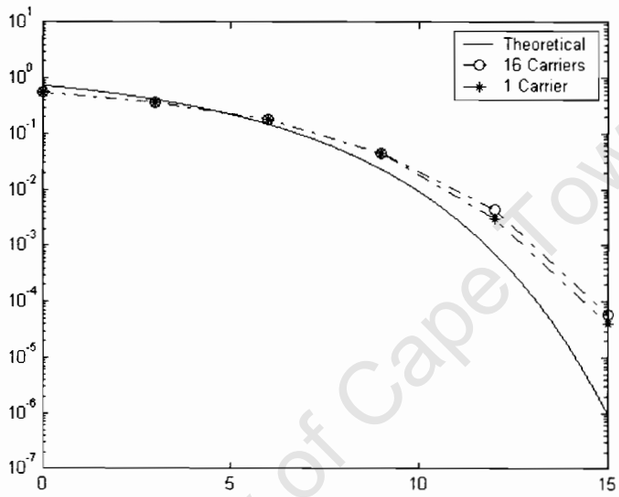

Figure 7.9: Error Simulation Results for OFDM 16-Carrier System with Channel and AWGN

It can be seen from the graph in Figure 7.9 that by reducing the number of carriers to 16, the SER now approaches that for a single carrier system. The effect is to reduce the overall data rate, but this is necessary in order to achieve acceptable error performance.

Chapter 8

Conclusions

The final chapter considers the original aims of the thesis and discusses their success or failure in the light of the theory and simulations laid out in previous chapters. A final basic specification for the system is given. The last section gives a summary of the aims and conclusions and concludes with some comments on the use of OFDM in packet radio.

8.1 Initial Aims

The initial aims of the thesis are summarised as follows:

- Produce an initial system specification based on the theory behind OFDM systems.
- Produce a software model that could be used to investigate the use of OFDM in packet radio.
- Determine whether or not companding could be used to reduce the PAPR in the system.
- Produce a final basic system specification

The achievement of these aims will be discussed in the following sections.

8.2 Achievement of Aims

8.2.1 Initial Specification

An initial specification for the model was generated in Chapter 2 and is shown in Table 8.1.

Available Bandwidth	8 kHz
Modulation Scheme	16-QAM
Bits per Symbol (bps)	4 bps
Sample Rate	48000 samples/s
FFT Length	128
No. of Carriers	20
Symbol Rate	375 symbols/s
Symbol Period	2.67 ms
Data Rate	30000 bps

Table 8.1: Initial Specification

8.2.2 OFDM Software Model

The development of the software model using Simulink was discussed in Chapters 3, 4 and 5. The performance of the model was examined in Chapter 7 using probability of SER and compared to theoretically expected performance. Single channel and multi-channel simulations were run using the transmitter model and the receiver model with AWGN and their performance compared to the theoretical ideal. It was found that the system performed as expected (Chapter 7.2) when compared to the theoretical performance. Although the SER at higher SNR could have been improved, it was felt that the model would be able to provide a basis to evaluate the use of OFDM in a packet radio system.

The full system was then simulated using the channel with AWGN, again using single and multi-channel systems. The performance of this system is shown in Chapter 7.4. Initial simulations showed that the performance of the 20-channel system was poor compared to that of the theory. Using the model it was determined that the number of channels would have to be reduced to 16 in order to maintain acceptable error results.

Based on this, a basic system that models the use of OFDM in a packet radio environment has been achieved.

8.2.3 Use of A-law Companding

The use of A-law compression and expanding was discussed in Chapter 6. In this chapter the basic theory behind companding was discussed, and a simple simulation using Matlab showed the effect of companding on a sinusoidal signal. It was shown that odd signal harmonics are generated in the companding process.

The performance simulation of a single channel and 20-channel companded system were measured in Chapter 7. The results showed that the single channel system did not perform well at low SNR and that the multi-channel system did not perform well at all.

For this reason, companding is not recommended for this system.

8.2.4 Final specification

The final specification for the system is given in Table 8.2. This specification is based on the original specification and was modified according to the characteristics of the channel model (Chapter 6) and the SER performance (Chapter 7).

Parameter	Specification
Available Bandwidth	8 kHz
Modulation Scheme	16-QAM
Bits per Symbol (bps)	4 bps
Sample Rate	48000 samples/s
FFT Length	128
No. of Carriers	16
Symbol Rate	363 symbols/s
Symbol Period	2.75 ms
Data Rate	23232 bps
Companding	Not Recommended

Table 8.2: Final System Specification

8.3 Summary

The chapter concludes with the following summary:

- A basic specification for the OFDM was generated in Chapter 2.
- A suitable software model was developed in Chapters 3,4 and 5 and its performance confirmed using simulated SER rates in Chapter 7.
- The use of A-law companding was investigated using SER simulations in Chapter 7. A-law companding is not recommended for this system.
- A final basic specification was generated in Chapter 8.

8.4 OFDM Use with Packet Radio

The simulations have shown that with the specifications laid down in the previous section, the maximum bit rate through the system would be approximately 23 kbps.

This value of data rate seems to be close to the limit for the proposed channel, although theoretically it could be 32 kbps.
The use of OFDM in such a bandlimited environment where the number of carriers is small, in this case 16, would not be the most efficient way to construct the system. Principle component filter banks, for example, are more efficient in the synthesis and analysis of multi-carrier systems for carrier numbers less than 32 [28].

The system still falls short of the 56 kbps that can be achieved over landline connections. Even although the 23 kbps is an increase over the types of systems still available, it is my opinion that the increase in the data rate would be marginal considering the added complexity of the OFDM system.

References

[1] G. Jones. *Introduction to Packet Radio*. URL : http:// www.tapr.org/tapr/html/pktfaq.html, Tucson Amateur Packet Radio, October 1996.

[2] G. H. Woodward, C. L. Hutchinson, P. L. Rinaldo *et al*. *The Radio Amateurs Handbook*. Sixty-First Edition, American Radio Relay League, 1984

[3] E.B. Carne. *Telecommunications Primer : Signals, Building Blocks and Networks*. Prentice Hall PTR, 1995.

[4] M Curtis, WD6EHR. *9600 Baud Packet Handbook*. URL : ftp//ftp.tapr.org/tapr/general/9600baud/96man2x0.txt. Version 2.0, June 13, 1992.

[5] B. McLarnon, VE3JF. *Equipment Options for Medium and High-Speed Packet Radio*. URL : http//hydra.carlton.ca/articles/hispeed/html. September 1996.

[6] J. Miller, G3RUH. *9600 Baud Packet Radio Modem Design*. Papers of ARRL 7th Computer Networking Conference (US), pp 135-140, October 1998.

[7] J. Miller, G3RUH. *Higher Speeds With the G3RUH 9600 Baud Packet Radio Modem*. August 1993.

[8] D. A. Heatherington, WA4DSY. *A 56 Kilobaud RF Modem.* Proceedings of the 6th Computer Networking Conference, pp 65-75, August 1987

[9] D. A. Heatherington. *The WA4DSY 56 Kilobaud Modem, A Major Redesign*. URL : http//www.wa4dsy.radio.org/56kb/56kpaper.html.

[10] B. McLarnon, VE3JF. *VHF/UHF/Microwave Radio Propagation : A Primer for Digital Experimenters* .
URL: http//www.tapr.org/tapr/html/ve3jf.dcc97/ve3jf.dcc97.html.

[11] T. McDermott, B. Stricklin and B. Reed. *An Amateur 900 MHz Spread Spectrum Radio Design*. Tucson Amateur Packet Radio Corporation.

[12] R.W.Chang, *High Speed Multi-channel Data Transmission With Bandlimited Orthogonal Signals*. Bell Systems Tech. J. Vol. 45, pp 1775-1796, December 1966

[13] B.R.Saltzberg, *Performance of an Efficient Parallel Data Transmission System*. IEEE Trans. Commun. Technol. Vol. COM-15, pp 805-811, December 1967.

[14] S.B. Weinstein, P.M. Ebert, *Data Transmission by Frequency Division Multiplexing Using the Discrete Fourier Transform*. IEEE Trans. Commun. Vol. 19(5), pp 628-634, October 1971.

[15] S.Hirosaki. *An Orthogonally Multiplexed QAM System Using The Discrete Fourier Transform*. IEEE Trans. Commun. Vol. COM-29, pp 982-989, July 1981.

[16] M.S. Zimmermann, A.L. Kirsch, *The AN/GSC-10/KATHRYN/ Variable Rate Data Modem for HF Radio*. IEEE Trans. Commun. Technol. Vol.CCM-15, pp 197-204, April 1967.

[17] T. Keller, L. Piazzo, P. Mandarini, L. Hanzo, *OFDM Synchronisation Techniques for Frequency Selective fading Channels*. IEEE Journal on Selected Areas in Commun. Vol. 19, No.6, pp 999-1008, June 2001.

[18] D. J. G. Mestdagh, P.M.P. Spruyt, *A Method to Reduce the Probability of Clipping in DMT-Based Transceivers*. IEEE Trans. Commun. Vol. 4 No. 10, pp 1234-1238, October 1996.

[19] L.J. Cimini, Jr., *Analysis and Simulation of a Digital Mobile Channel Using Orthogonal Frequency Division Multiplexing*. IEEE Trans. Commun. Vol. COM-33, No.7, pp 665-675, July 1985.

[20] I. Korn, *Effect of Intersymbol and Quadrature Channel Interference on Error Probability of 16-ary Offset Quadrature Amplitude Modulation with Sinusoidal and Rectangular Shaping*. IEEE Trans. Commun. Vol. COM-31, No.2, pp 264-269 February 1983.

[21] The MathWorks, *Simulink. Model-Based and System-Based Design. Using Simulink Ver.5*. The MathWorks Inc. Natick, MA. 2003.

[22] The MathWorks, *Signal Processing Toolbox Users Guide*. The MathWorks Inc. Natick, MA. 2000

[23] J.G. Proakis, M. Salehi, *Contemporary Communications Systems Using Matlab*. PWS Publishing Company, 20 Park Plaza, Boston, MA 02116-4324. 1998.

[24] The MathWorks, *Communications Toolbox Users Guide*. The MathWorks Inc. Natick, MA. 1997.

[25] R.E. Ziemer, W.H. Tranter, *Principles of Communications. Systems, Modulation and Noise*. Houghton Mifflin Company, Boston. 1985.

[26] S. Haykin, *An Introduction to Analog and Digital Communications*. John Wiley and Sons. 1989.

[27] Xianbin Wang, Tjeng Thiang Tjhung, Chun Sum Ng, Ashaf Ali Kassim, *On the SER Analysis of A-Law Companded OFDM Systems*. Proc. IEEE GLOBECOM, 2000, pp 756-760, November 2000.

[28] J.G. Proakis, *Digital Communications*. McGraw Hill International. Fourth Edition. 2001.

[29] Xiadong Li, Leonard J. Cimini, *Effects of Clipping and Filtering on the Performance of OFDM*. IEEE Commun. Letters, Vol2, No5, pp 131-133, May 1998.

[30] V. Tarokh, H. Jafarkhani, *On the Computation and Reduction of the Peak-to-Average Power Ratio in Multicarrier Communications*. IEEE Trans. Commun. Vol.48, No.1, pp 37-44, January 2000.

[31] W. Henkel, B. Wagner, *Another Application for Trellis Shaping: PAR for DMT (OFDM)*. IEEE Trans. Commun. Vol. 48. No.9, pp 1471-1476, September 2000.

[32] Wayne Tomasi, *Advanced Electronic Communications Systems*. Third Edition. Prentice-Hall Inc. Engelwood Cliffs, NJ 07632. 1994.

[33] I. Kalet, *The Multitone Channel*. IEEE Trans. Commun. Vol. COM-37, pp. 119 - 124, February 1989.

Appendix A

Software Listings

A.1 Chapter 2

The following is the listing for the Matlab m-file *tones.m*.

```
function [A]=tone();
%Function to generate a range of possible carrier frequencies
%and determine the corresponding data rate.
%Parameters maxfreq=8kHz, bits per symbol=4.
hold off
maxfreq=8;          %Initiallisation
bpsym=4;
sym_rate=[];
num_of_tones=[];
kbps=[];

space=0.1:0.001:maxfreq;      %Generates carrier frequencies.

deltafreq=space;

for n=1:length(space);

   num=1;

   startfreq=space(n);

   increment=deltafreq(n);

   newtones=startfreq;

    while newtones<(maxfreq-increment)
     newtones=newtones+increment;
```

```
    num=num+1;
    fundamental(n)=space(n);
    sym_rate(n)=startfreq*num;
     num_of_tones(n)=num;
     kbps(n)=startfreq*num*bpsym;

   end

end

A=[ fundamental;
   sym_rate;
  num_of_tones;
  kbps];

%hold on
%plot(space,sym_rate)
%plot(space,num_of_tones,'r-')
%plot(space,kbps,'g-')
```

A.2 Chapter 7

```
%function [theo_err_prb]= proberr()

% MATLAB script for Illustrative Problem 6, Chapter 7.

SNRindB2=0:0.01:15;
M=16;
k=log2(M);

for i=1:length(SNRindB2),
 SNR=exp(SNRindB2(i)*log(10)/10);       % Eavb/N0
 % theoretical symbol error rate
 theo_err_prb(i)=4*Qfunct(sqrt(3*k*SNR/(M-1)));
end;
% Plotting commands follow

semilogy(SNRindB2,theo_err_prb);
```

The following function is taken from [23].

```
function [y]=Qfunct(x)
% [y]=Qfunct(x)
%              QFUNCT  evaluates the Q-function.
%              y = 1/sqrt(2*pi) * integral from x to inf of exp(-t^2/2) dt.
%              y = (1/2) * erfc(x/sqrt(2)).
y=(1/2)*erfc(x/sqrt(2));
```

Appendix B

Channel Measurement

As stated at the beginning of Chapter 5, the channel simulation model is based on measurements taken from an Agilent Technologies HP8920A RF Communications Test Set. Figure B.1 shows the block diagram of the test setup.

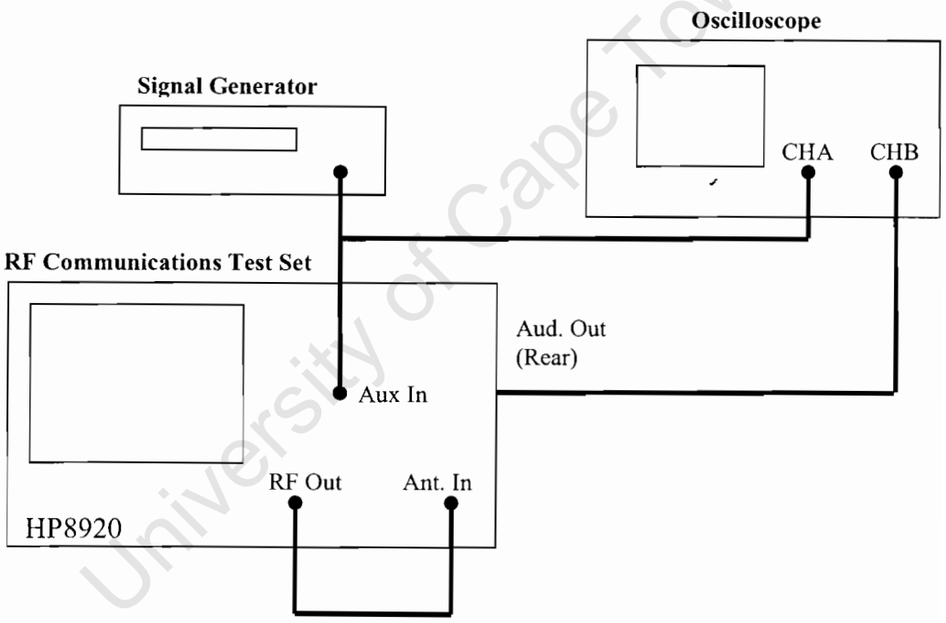

Figure B.1: Block Diagram of Channel Model Test Setup

Frequency (kHz)	Amplitude (mV_{p-p})	Delay (µs)
1	70.6	72
2	72.5	76
3	71.9	72
4	70.6	74
5	70.6	78
6	68.8	81
7	61.9	80
8	46.9	86
9	35.6	84
10	29.4	84
11	20.6	83
12	15.0	77
13	12.8	71

Table B.1: Channel Measurement Data for HP8920A

Parameter	Value
Carrier Frequency	145 MHz
Deviation	4 kHz
Output Level	-20 dBm
Pre-emphasis	None
De-emphasis	None
Test Signal Amplitude	397 mV_{p-p}

Table B.2: HP8920A Settings

Appendix C

Simulation Results

The following are tables of the SER tests carried out in Chapter 7. All simulations were run for 100 000 symbols.

7.2 OFDM Model with Single and Multi-Carriers, No Channel

Input Signal Power for AWGN block, 6.667e-03 W.

SER, dB	1 Carrier SER	20 Carrier SER
0	0.555	0.557
3	0.376	0.382
6	0.1818	0.1830
9	0.04687	0.04691
12	0.00324	0.00333
15	0.00004	0.00005

Table C.1: SER Rates for Chapter 7.2

7.3 OFDM Model with Companding, No Channel

SER, dB	1 Carrier SER	20 Carrier SER
0	0.71	0.868
3	0.56	0.827
6	0.40	0.745
9	0.21	0.605
12	058	0.391
15	0.005	0.169

Table C.2: SER Rates for Chapter 7.3

7.4 OFDM with Channel and AWGN

Input signal power for AWGN block, 210e-06 W

SER, dB	1 Carrier SER	20 Carrier SER
0	0.5532	0.5675
3	0.3727	0.3955
6	0.1775	0.2089
9	0.04546	0.07365
12	0.003	0.02037
15	4e-05	0.00731

Table C.3: SER Rates for Chapter 7.4

SER, dB	16 Carrier SER
0	0.5499
3	0.3709
6	0.1784
9	0.04576
12	0.00445
15	6e-05

Table C.4: SER Rates for Chapter 7.4, 16 Carrier